THE JOURNAL OF BIOLOGICAL CHEMISTRY VOL. 287, NO. 15, pp. 12250–12266, April 6, 2012

Connexin 43 Hemichannels Contribute to Cytoplasmic Ca^{2+} Oscillations by Providing a Bimodal Ca^{2+}-dependent Ca^{2+} Entry Pathway*[S]

Received for publication, September 1, 2011, and in revised form, February 16, 2012 Published, JBC Papers in Press, February 20, 2012, DOI 10.1074/jbc.M111.299610

Marijke De Bock[‡], Nan Wang[‡], Melissa Bol[‡], Elke Decrock[‡], Raf Ponsaerts[§], Geert Bultynck[§], Geneviève Dupont[¶1], and Luc Leybaert[‡2]

From the [‡]Department of Basic Medical Sciences, Physiology Group, Ghent University 9000 Ghent, Belgium, [§]Department of Molecular Cell Biology, Laboratory of Molecular and Cellular Signaling, KULeuven, 3000 Leuven, Belgium, and [¶]Theoretical Chronobiology Unit, Université Libre de Bruxelles, 1050 Brussels, Belgium

Background: Connexin hemichannels are Ca^{2+}-permeable plasma membrane channels that are controlled by $[Ca^{2+}]_i$; therefore, they may contribute to Ca^{2+} oscillations.
Results: Ca^{2+} oscillations triggered by bradykinin in connexin-expressing cells were inhibited by blocking hemichannel opening or by preventing their closure at high $[Ca^{2+}]_i$; ATP-triggered oscillations were unaffected.
Conclusion: Hemichannels contribute to oscillations by controlling Ca^{2+} entry.
Significance: Hemichannels together with $InsP_3$ receptors help shape agonist-induced Ca^{2+} oscillations.

Many cellular functions are driven by changes in the intracellular Ca^{2+} concentration ($[Ca^{2+}]_i$) that are highly organized in time and space. Ca^{2+} oscillations are particularly important in this respect and are based on positive and negative $[Ca^{2+}]_i$ feedback on inositol 1,4,5-trisphosphate receptors ($InsP_3Rs$). Connexin hemichannels are Ca^{2+}-permeable plasma membrane channels that are also controlled by $[Ca^{2+}]_i$. We aimed to investigate how hemichannels may contribute to Ca^{2+} oscillations. Madin-Darby canine kidney cells expressing connexin-32 (Cx32) and Cx43 were exposed to bradykinin (BK) or ATP to induce Ca^{2+} oscillations. BK-induced oscillations were rapidly (minutes) and reversibly inhibited by the connexin-mimetic peptides ^{32}Gap27/^{43}Gap26, whereas ATP-induced oscillations were unaffected. Furthermore, these peptides inhibited the BK-triggered release of calcein, a hemichannel-permeable dye. BK-induced oscillations, but not those induced by ATP, were dependent on extracellular Ca^{2+}. Alleviating the negative feedback of $[Ca^{2+}]_i$ on $InsP_3Rs$ using cytochrome *c* inhibited BK- and ATP-induced oscillations. Cx32 and Cx43 hemichannels are activated by <500 nM $[Ca^{2+}]_i$ but inhibited by higher concentrations and CT9 peptide (last 9 amino acids of the Cx43 C terminus) removes this high $[Ca^{2+}]_i$ inhibition. Unlike interfering with the bell-shaped dependence of $InsP_3Rs$ to $[Ca^{2+}]_i$, CT9 peptide prevented BK-induced oscillations but not those triggered by ATP. Collectively, these data indicate that connexin hemichannels contribute to BK-induced oscillations by allowing Ca^{2+} entry during the rising phase of the Ca^{2+} spikes and by providing an OFF mechanism during the falling phase of the spikes. Hemichannels were not sufficient to ignite oscillations by themselves; however, their contribution was crucial as hemichannel inhibition stopped the oscillations.

Ca^{2+} is a universal and versatile intracellular messenger controlling a large variety of basic cellular functions that include fertilization, gene expression, cell differentiation, exocytosis, muscle contraction, cell survival, and cell death (1, 2). Ca^{2+} is released from the endoplasmic reticulum (ER),[3] the cell's major Ca^{2+} store, after activation of $G\alpha_q$-protein-coupled receptors (GPCR) on the plasma membrane with subsequent activation of phospholipase C_β (PLC_β), hydrolysis of phosphatidylinositol 4,5-bisphosphate, and production of inositol 1,4,5-trisphosphate ($InsP_3$). Stimulation of $InsP_3$ receptors ($InsP_3Rs$) on the ER membrane triggers the release of ER Ca^{2+}, thereby increasing the cytosolic Ca^{2+} concentration ($[Ca^{2+}]_i$). $[Ca^{2+}]_i$ elevation is followed by a recovery phase that is mediated by Ca^{2+} sequestration back into the ER lumen through sarcoplasmic/endoplasmic Ca^{2+} ATPases and by Ca^{2+} extrusion out of the cell through plasma membrane Ca^{2+} ATPases (3, 4). This is followed by store-operated Ca^{2+} entry (SOCE) to replenish the ER with Ca^{2+} and attain pre-spike ER Ca^{2+} content (5). Physiological Ca^{2+} signals can take the form of a single, transient elevation in $[Ca^{2+}]_i$ but may also appear as repeated $[Ca^{2+}]_i$ transients, called Ca^{2+} oscillations (2, 6). The simplest model of Ca^{2+} oscillations is based on positive and negative modulatory

* This work was supported by the Institute for the Promotion of Innovation of Science and Technology in Flanders (IWT Vlaanderen) Grant 63352 (to M. D. B.), the Fund for Scientific Research Flanders (FWO) grants G.0140.08 and 3G.0134.09 (to L. L.) and G.0298.11 (L. L. and G. B.), and the Interuniversity Attraction Poles Program (Belgian Science Policy) P6/31 (to L. L.) and P6/28 (to G. B.).
[S] This article contains supplemental Fig. S1.
[1] Maître de Recherche at the Belgian Fonds de la Recherche Scientifique.
[2] To whom correspondence should be addressed: Dept. of Basic Medical Sciences, Physiology group, Faculty of Medicine and Health Sciences, Ghent University, De Pintelaan 185, Bldg. B (Rm. 310), 9000 Ghent, Belgium. Tel.: 32-9-332-33-66; Fax: 32-9-332-30-59; E-mail: Luc.Leybaert@UGent.be.

[3] The abbreviations used are: ER, endoplasmic reticulum; AUC, area under the curve; BK, bradykinin; CT, C-terminal peptide; Cx, connexin; CytC, cytochrome *c*; DTR, dextran Texas Red; GPCR, G-protein-coupled receptor; $InsP_3$, inositol 1,4,5 trisphosphate; $InsP_3R$, $InsP_3$ receptor; MDCK, Madin-Darby canine kidney; PI, propidium iodide; PLC, phospholipase C; RT, room temperature; SOCE, store-operated Ca^{2+} entry; Cbx, carbenoxolone; HBSS, Hanks' balanced salt solution; PPADS, Pyridoxalphosphate-6-azophenyl-2′,4′-disulfonic acid.

effects of Ca^{2+} on the open probability of $InsP_3R$ channels, which display a typical bell-shaped dependence (7, 8). When $[Ca^{2+}]_i$ is below a certain threshold (~300 nM), Ca^{2+} potentiates $InsP_3$-triggered Ca^{2+} release (7), resulting in Ca^{2+}-induced Ca^{2+} release (9). A further rise in $[Ca^{2+}]_i$ above this level results in negative feedback, marking the start of the decaying phase of the Ca^{2+} spike (7). After restoration of the ER Ca^{2+} content (by sarcoplasmic/endoplasmic Ca^{2+} ATPase pumps and SOCE) the cycle repeats to induce the next Ca^{2+} spike. An important condition for Ca^{2+} oscillations to occur is the necessity for kinetic differences between positive and negative Ca^{2+} feedback, which means the positive feedback action should be faster than the negative one (8, 10–12), a condition that is fulfilled for $InsP_3R$ channels (13, 14). Continued Ca^{2+} oscillations necessitate a slightly elevated intracellular $InsP_3$ concentration that sets a certain degree of Ca^{2+} excitability of $InsP_3R$ channels, making them sensitive to small local Ca^{2+} increases that can fire the next Ca^{2+} spike through Ca^{2+}-induced Ca^{2+} release (10). When the $InsP_3$ concentration is elevated consequent to stronger GPCR stimulation, the oscillation frequency generally increases (10, 15). In addition, the intracellular $InsP_3$ concentration is not solely determined by the level of GPCR stimulation but may also be influenced by direct or indirect feedback actions of $[Ca^{2+}]_i$ on Ca^{2+}- or PKC-sensitive PLC isoforms (δ, ζ, η or β, γ isoforms, respectively) (16, 17), thereby generating oscillations in the $InsP_3$ concentration. These $InsP_3$ oscillations may modulate the Ca^{2+} oscillations (by augmenting Ca^{2+}-induced Ca^{2+} release (11)) but may also take the lead and provide the primary driving force for the Ca^{2+} oscillations (18), depending on the GPCRs involved. Additionally, other feedback actions on the $InsP_3$ metabolism (11, 19) and on Ca^{2+} entry (20–24) provide supplementary tools to modulate and shape the oscillatory signal (25).

Evidence is accruing that connexin channels play a role in Ca^{2+} oscillations. Connexins form two kinds of channels, hemichannels and gap junction channels, the latter resulting from the head-to-head interaction of two hemichannels. Gap junction channels connect the cytoplasm of adjacent cells, whereas unapposed hemichannels, when open, link the cytoplasm with the extracellular fluid. Both types of channels are permeable to substances with a molecular mass below 1–1.5 kDa (26, 27). Kawano *et al.* (28) reported that octanol, a nonspecific connexin channel blocker, inhibited spontaneous Ca^{2+} oscillations in human mesenchymal stem cells. This work suggested the opening of hemichannels followed by ATP diffusing out of the cell and acting in an autocrine way on plasma membrane $P2Y_1$ receptors, thereby activating PLC_β and generating $InsP_3$. Verma *et al.* (29) reported that ^{43}Gap26 and $^{37/43}$Gap27, two synthetic peptides that mimic short sequences in, respectively, the first extracellular loop of connexin 43 (Cx43) and the second extracellular loop of Cx37/Cx43, inhibited Ca^{2+} oscillations in connexin-expressing HeLa cells and in cardiac myocytes. ^{43}Gap26 and $^{37/43}$Gap27 peptides are inhibitors of Cx43 gap junctions and have been reported to inhibit Cx43 hemichannels with faster kinetics (30–33). Verma *et al.* (29) proposed that Gap inhibition of Ca^{2+} oscillations was mediated by reducing Ca^{2+} entry via hemichannels thereby affecting ER Ca^{2+} release. We recently reported that $^{37/43}$Gap27 inhibits bradykinin (BK)-triggered Ca^{2+} oscillations in blood-brain barrier endothelial cells and thereby prevents a subsequent increase in barrier permeability (34). In addition to the fact that hemichannel-mediated ATP release and Ca^{2+} entry may play a role in Ca^{2+} oscillations, hemichannel opening is controlled by $[Ca^{2+}]_i$ (35–37). Because hemichannels both influence and are influenced by $[Ca^{2+}]_i$, we examined the mechanisms by which hemichannels contribute to Ca^{2+} oscillations. We specifically aimed to determine whether hemichannel-$[Ca^{2+}]_i$ interactions constitute a mechanism supporting oscillatory activity in a manner analogous to the $InsP_3R$-$[Ca^{2+}]_i$ link by using tools that selectively target either $InsP_3Rs$ or connexin channels. We found that hemichannels contribute to $InsP_3R$-based oscillations by providing a Ca^{2+} entry pathway and by shutting down this Ca^{2+} entry pathway by inhibiting hemichannel activity when $[Ca^{2+}]_i$ increases above ~500 nM. This contribution of hemichannels was essential as the Gap peptides blocked the BK-induced oscillations. Hemichannels were not involved in ATP-induced Ca^{2+} oscillations, indicating that they may help in shaping distinct Ca^{2+} response patterns to different agonists.

EXPERIMENTAL PROCEDURES

Cell Culture—MDCK cells (up to passage 15) and C6-glioma cells stably transfected with Cx43 (C6Cx43), Panx1 (C6Panx1), or Panx1-Myc (C6Panx1-Myc) (C6 were kindly provided by Dr. Christian C. Naus, University of British Columbia) were maintained in Dulbecco's modified Eagle's medium/Ham's F-12 (1:1) supplemented with 10% fetal calf serum (FCS) and 2 mM glutamine, 10 units/ml penicillin, 10 μg/ml streptomycin, and 0.25 μg/ml Fungizone (all from Invitrogen) at 37 °C and 5% CO_2. Rat brain endothelial (RBE4) cells were maintained in α-minimal essential medium/Ham's F-10 supplemented with 10% FCS, 2 mM L-glutamine, 300 μg/ml G418 (Invitrogen), and 1 ng/ml human recombinant basic fibroblast growth factor (Roche Diagnostics). MDCK and RBE4 cells were grown on collagen-coated recipients (rat-tail collagen, Roche Diagnostics).

Chemicals and Reagents—Arachidonyl trifluoromethyl ketone, 4-bromo-A23187, ATP, apyrase grade VI and VII, bradykinin, carbenoxolone (Cbx), cytochrome *c* (CytC) from equine heart, digitonin, EGTA, 8-(*p*-sulfophenyl)theophylline, and staurosporine were purchased from Sigma. 1,2-Bis(2-aminophenoxy) ethane-*N*,*N*,*N*′,*N*′-tetraacetic acid tetrakis-acetoxymethyl ester (BAPTA-AM), calcein-AM, 5-carboxyfluorescein diacetate-AM, 10-kDa dextran Texas Red (DTR), 10-kDa dextran fluorescein, D-*myo*-inositol 1,4,5-trisphosphate, $P^{4(5)}$-1-(2-nitrophenyl)ethyl ester ("caged $InsP_3$"), fluo3-AM, fura2-AM, Hoechst 33342, Mitotracker Green FM, *o*-nitrophenyl-EGTA-AM ("Caged Ca^{2+}"), propidium iodide (PI), RhodFF-AM and thapsigargin were from Molecular probes (Invitrogen). Xestospongin-C and U73122 were from Tocris Bioscience (Bristol, UK). ^{32}Gap27 (SRPTEKTVFT, amino acids 182–191 in the second extracellular loop of Cx32), ^{43}Gap26 (VCYDKSFPISHVR, amino acids 64–76 in the first extracellular loop of Cx43), CT9 (RPRPDDLEI, last 9 amino acids of the C-terminal tail of Cx43), CT9ΔI (RPRPDDLE), the reversed CT9 peptide ($CT9^{Rev}$, IELDDPRPR), YGRKKRRQRRR-CT9 (Tat-CT9), and Tat-$CT9^{Rev}$ were synthesized by LifeTein at

>80% purity. The C-terminal peptide IP_3RCYT, corresponding to amino acids 2621–2636 of $InsP_3$R1 (DNKTVTFEEHIKEEHNC) (38), was a kind gift of Dr. Darren F. Boehning (University of Texas Medical Branch).

Ca^{2+} Imaging—MDCK cells were seeded onto 18-mm-diameter glass coverslips (Knittel Glaser, Novolab, Geraardsbergen, Belgium), and experiments were performed at subconfluency the next day. The cells were loaded with 10 μM fluo3-AM in HBSS-Hepes (1 mM $CaCl_2$, 0.81 mM $MgSO_4$, 13 mM NaCl, 0.18 mM Na_2HPO_4, 5.36 mM KCl, 0.44 mM KH_2PO_4, 5.55 mM D-glucose, and 25 mM Hepes) for 1 h at room temperature (RT). After 1 h, coverslips were washed and then left for an additional 30 min at RT in HBSS-Hepes to allow for de-esterification. Cells were thereafter transferred to an inverted epifluorescence microscope (Eclipse TE 300, Nikon Belux, Brussels, Belgium) equipped with a superfusion system that allowed changing the bath solution within ~1 min (bath volume ~300 μl). Superfusion was switched off during the registration of oscillatory activity. Images were taken every second with a ×40 oil-immersion objective and an electron-multiplying CCD camera (Quantem 512SC, Photometrics, Tucson, AZ). We used a Lambda DG-4 filterswitch (Sutter Instrument Company, Novato, CA) to deliver excitation at 482 nm and captured emitted light via a 505-nm long-pass dichroic mirror and a 535-nm bandpass filter (35-nm bandwidth). Cells were loaded with fura2-AM (5 μM) in a similar manner. Excitation was alternated between 340 and 380 nm at a rate of one image pair every second. Emitted light was captured using a 430-nm long-pass dichroic mirror and a 510-nm bandpass-filter (40-nm bandwidth). Fura2 *in situ* calibration was performed in zero Ca^{2+} medium (10 mM EGTA) containing 10 μM A23187 (R_{min}) and a saturating Ca^{2+} solution (10 mM $CaCl_2$) containing 40 μM digitonin (R_{max}). $[Ca^{2+}]_i$ was calculated from $K_d \cdot Q \cdot [(R - R_{min})/(R_{max} - R)]$, where R is the F_{340}/F_{380} ratio, Q is F_{min}/F_{max} at 380 nm, and K_d 224 nM (39). Mitochondrial Ca^{2+} measurements were performed with the mitochondrial Ca^{2+} indicator RhodFF as we described previously (40). MDCK cells were loaded with RhodFF-AM (5 μM) for 1 h at RT followed by 30 min of de-esterification. Imaging was performed in a similar manner as fluo3 imaging but with excitation at 556 nm and long-pass filtering at 590 nm. A punctate distribution that matches the distribution of Mitotracker Green (100 nM, 1 h, RT) confirmed the mitochondrial localization of the dye (supplemental Figs. S1). Recordings and analysis were done with custom-developed QuantEMframes and Fluoframes software written in Microsoft Visual C^{++} 6.0. Oscillatory activity was recorded in a 10-min observation window, and only Ca^{2+} spikes minimally 10% above baseline were considered in the analysis. To calculate the percentage of oscillating cells, an oscillating cell was defined as a cell displaying at least two Ca^{2+} spikes subsequent to the initial spike. The percentage of cells oscillating was calculated relative to the total number of cells in view. The oscillation frequency is the average frequency of all cells in view including non-oscillating cells.

Electroporation Loading—MDCK cells were loaded with CytC or CT peptides by electroporation. Cells, seeded the day before the experiment, were rinsed with a low conductivity electroporation buffer and placed on the microscope stage. Thereafter, a small volume (10 μl) of CytC (3 μM)/DTR (100 μM) or CT9 peptide (300 μM)/PI (12 μM) dissolved in electroporation buffer was added to a parallel wire Pt-Ir electrode positioned 400 μm above the cells. DTR (10 kDa) or PI (668 Da) have molecular masses approaching that of CytC (12 kDa) or CT9 (1 kDa), respectively, and were added to visualize the electroporated cells. In experiments using the Ca^{2+} dye RhodFF, we visualized the CytC-loaded zone with 10-kDa dextran fluorescein. The IP_3RCYT peptide (15 μM) was added to the CytC (3 μM) solution (see above) 30 min before electroporation to allow for interaction. Electroporation was performed after fluo3-AM loading with 50-kHz bipolar pulses at a field strength of 1000 V/cm, applied as 15 trains of 10 pulses of 2-ms duration each (41, 42). Electroporation did not result in loss of fluo3/fura2/RhodFF from the cells.

Caged Compound Loading and Photoliberation—Cells seeded on coverslips the day before the experiment were electroporated with cell-impermeant, caged $InsP_3$ (30 μM), and DTR (100 μM) as described above. Caged Ca^{2+} was loaded into the cells by ester-loading, similar to the Ca^{2+}-sensitive dyes. Thereafter, the coverslips were transferred to an inverted epifluorescence microscope. Photoliberation of $InsP_3$ was done by spot (20 μm diameter) illumination with 1-kHz pulsed UV light (349 nm UV laser Explorer, Spectra-Physics, Newport, Utrecht, The Netherlands) applied during 20 ms (20 pulses of 90 μJ energy measured at the entrance of the microscope epifluorescence tube). For uncaging of Ca^{2+} we applied UV illumination with different flash durations.

Hemichannel Assays—Hemichannel opening was investigated by calcein (623 Da) release, which is based on the efflux of the preloaded dye via open hemichannels (43). Subconfluent cultures of MDCK cells grown on glass coverslips (18 mm diameter), were preloaded with 50 μM calcein-AM in HBSS-HEPES for 1 h at RT. Subsequently, the remaining calcein-AM was removed; cells were left for an additional 30 min at RT in HBSS-Hepes to allow the AM ester to de-esterify and were then transferred to the stage of an inverted epifluorescence microscope. For analysis, we measured the decrease in calcein fluorescence in function of time. The first 5 min, baseline leakage in HBSS-Hepes was measured (control); thereafter, the trigger solution was added, and efflux of calcein was further evaluated. The slope of the curve, calculated by linear regression, was used as a parameter describing the loss of dye in time. Calcein efflux in the presence of trigger is presented as % of control.

Gap Junction Dye Coupling Studies—Dye coupling via gap junctions was determined using fluorescence recovery after photobleaching. MDCK cell cultures were grown to confluence on 9.2 cm^2 Petri dishes (Techno Plastic Products, Trasadingen, Switzerland) and loaded with the gap junction-permeable fluorescent dye 5-carboxyfluorescein diacetate-AM (532 Da, 10 μM) in HBSS-Hepes for 1 h at RT. After de-esterification, cells were transferred to a custom-made video-rate confocal laser scanning microscope with a ×40 water immersion objective (CFI Plan Fluor) and a 488-nm laser excitation source (Cyan CW Laser, 488 nm, 100 milliwatt; Newport Spectra-Physics, Utrecht, The Netherlands). After 1 min of recording, the cell in the middle of the field was photobleached by spot exposure (1 s) to increased power of the 488 nm laser, and fluorescence recov-

ery, caused by dye influx from neighboring non-bleached cells, was recorded during an additional 5-min period. The fluorescence recovery trace was then analyzed for the recovery of the signal expressed relative to the starting level before photobleaching.

Ectonucleotidase Activity—Ectonucleotidase activity was assessed by measuring the breakdown of ATP added to the cells via the decline of luciferin/luciferase luminescence in the medium above the cells. MDCK and RBE4 cells were seeded at a density of 40,000 cells/cm^2 in 24-well plates. ATP (100 μM) together with an ATP bioluminescent assay mix (luciferin/luciferase, 625-fold dilution, Sigma) was prepared in ATP assay mix dilution buffer (Sigma). Photon flux was counted using a multilabel counter (Victor-3, type 1420, PerkinElmer Life Sciences). The time constant (τ) of the exponential luminescence decay was used as a parameter to express ectonucleotidase activity.

Apoptosis Assay—Annexin V staining detects the flip-flop of phosphatidylserine toward the outer plasma membrane leaflet that occurs during apoptosis. After electroporation with 10-kDa DTR (100 μM) and CytC (3 μM), cells were rinsed with PBS and incubated for 15 min (RT) with annexin V-FITC (1:50; Roche Diagnostics) and Hoechst 33342 (2 μg/ml) in annexin V buffer (140 mM NaCl, 5 mM $CaCl_2$, 10 mM HEPES, pH 7.4). The cultures were subsequently washed with PBS and transferred to a Nikon TE300 epifluorescence microscope, equipped with a ×10 objective (Plan Apo, NA 0.4, Nikon). Ten images inside the electroporation zone were taken, and annexin V-positive cells were counted. The number of apoptotic cells was expressed as the percentage of annexin V-positive cells relative to the total number of cells (determined by Hoechst 33342 staining).

siRNA Treatment—MDCK cells were seeded onto 18-mm diameter glass coverslips at a density of 20,000 cells/cm^2 and transfected the following day using Dharmafect1 lipid reagent (Dharmacon, Thermo Fisher Scientific). We used two siRNA duplexes (125 nM) directed against the canine Cx43 gene gja1 (siCx43–1, 5′-GUUCAAGUAUGGAAUUGAA-dTdT-3′; siCx43–2, 5′-UUCAAUUCCAUACUUGAAC-dTdT-3′). On day 3, medium was refreshed, and on day 4, cells were used for experiments. Transfection efficiency on day 3 was 52 ± 4.1% ($n = 11$), as determined with the fluorescent indicator siGLO. Control conditions were untreated cultures, mock-treated cultures (lipid reagent alone), and a negative control consisting of cultures transfected with a scrambled version of siCx43–1 (siCx43–1^{Scr}: 5′-GCGUAUAUAUGAGUAAGUA-dTdT-3′). All siRNA duplexes were synthesized and annealed by Eurogentec (Luik, Belgium) after selective designing against *Canis familiaris* and screening for off-target sequences using Batch RNAi selector (44).

Electrophoresis and Western Blot Analysis—For Western blots, cells were seeded in 75-cm^2 flasks. Total MDCK cell lysates were extracted with radioimmune precipitation assay buffer (25 mM Tris, 50 mM NaCl, 0.5% Nonidet P-40, 0.5% deoxycholate, 0.1% SDS, 1 mM DTT, 0.055 g/ml β-glycerol phosphate, 30 μl/ml phosphatase inhibitor mixture, and 20 μl/ml mini EDTA-free protease inhibitor mixture). For separation of Triton X-100 soluble (cytosol) and insoluble (membrane) fractions, cells were harvested in 1% Triton X-100 supplemented with 50 mM NaF and 1 mM Na_3VO_4, and centrifuged at 16,000 g for 10 min. The Triton X-100 insoluble pellets were resuspended in 1× Laemmli sample buffer. Protein concentration was determined using a Bio-Rad DC protein assay (Bio-Rad), and absorbance was measured with a 590-nm long-pass filter. Lysates were separated by electrophoresis over a 10% SDS-polyacrylamide gel and transferred to a nitrocellulose membrane (Amersham Biosciences). Membranes were subsequently blocked with TBS containing 5% nonfat milk and 0.1% Tween20. After blocking, blots were probed with rabbit anti-Cx43 antibody (Sigma), rabbit anti-Cx32 antibody (Sigma), rabbit anti-Cx26 antibody (Zymed Laboratories Inc., Invitrogen), rabbit anti-phospho-Cx43 (Ser(P)-368) (Cell Signaling Technology, Inc., Danvers, MA), rabbit anti-$P2X_7$ antibody (Alomone Labs, Jerusalem, Israel), anti-Panx1 antibody (a kind gift of Dr. Dale W. Laird, University of Western Ontario), and rabbit anti-β-tubulin antibody (Abcam, Cambridge, UK) as a loading control. Membranes were subsequently incubated with an alkaline phosphatase-conjugated goat anti-rabbit IgG antibody (Sigma), and detection was done using the nitro blue tetrazolium/5-bromo-4-chloro-3-indolyl-phosphate reagent (Zymed Laboratories Inc., Invitrogen). Quantification was done by drawing a rectangular window around the concerned band and determining the signal intensity using ImageJ software. Background correction was done by the same procedure applied to nitrocellulose membranes where protein was absent.

Statistical Analysis—Data are expressed as the mean ± S.E. with n giving the number of independent experiments. Multiple groups were compared by one-way analysis of variance and Bonferroni post-test, making use of Graphpad Instat software. Two groups were compared with an unpaired Student's t test and two-tail p value. Results were considered statistically significant when $p < 0.05$ (one symbol for $p < 0.05$, two for $p < 0.01$, and three for $p < 0.001$).

RESULTS

Concentration and $InsP_3$ Dependence of BK- and ATP-induced Ca^{2+} Oscillations—We first characterized BK- and ATP-induced Ca^{2+} oscillations in MDCK cells and determined the concentration dependence of the percentage of oscillating cells and of the oscillation frequency. We used non-confluent MDCK cell cultures to this purpose to limit the degree of gap junctional coupling. BK and ATP triggered an initial $[Ca^{2+}]_i$ transient followed by repetitive Ca^{2+} spikes (recorded over a 10-min period) with quite a different profile (Fig. 1, *A* and *B*). BK concentrations ranging from 0.05 to 100 μM all triggered Ca^{2+} oscillations in an invariable percentage of cells (~72%) and a similar oscillation frequency (~5 spikes/10 min, measured over all cells in view) (Fig. 1*C*). By contrast, oscillations triggered by ATP concentrations between 0.5 μM and 2 mM were characterized by a bell-shaped concentration-response curve for the percentage of oscillating cells and oscillation frequency (Fig. 1*D*). The maximum number of oscillating cells (89 ± 3.4%; $n = 5$) and the maximal oscillation frequency (13 ± 1.1 spikes/10 min; $n = 5$) were observed with 10 μM ATP. These markedly different patterns of concentration dependence indicate distinct oscillation mechanisms for ATP and BK. We chose 10 μM ATP (a concentration located between the two peaks

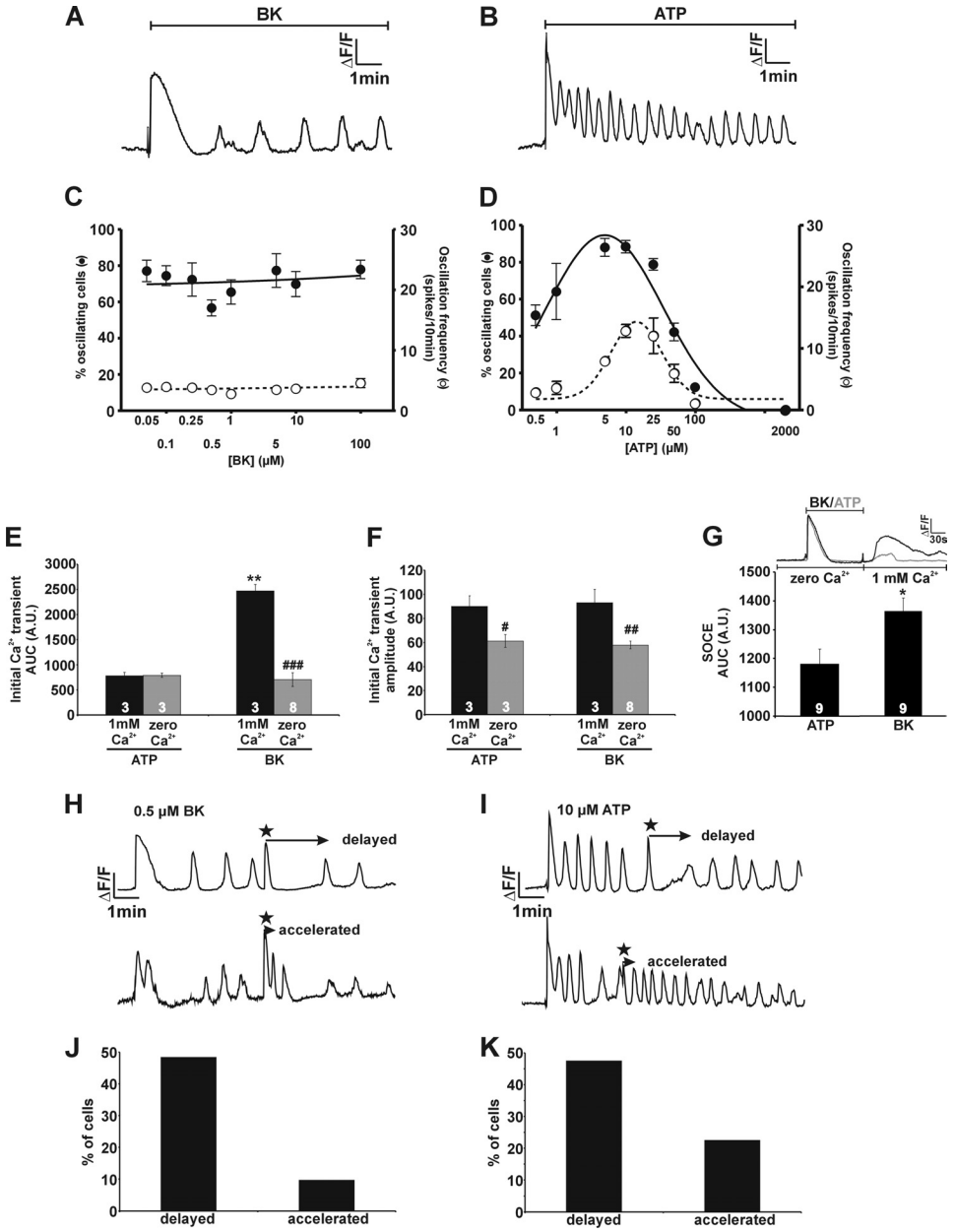

FIGURE 1. **Concentration dependence of Ca^{2+} oscillations triggered by BK and ATP.** *A* and *B*, representative traces demonstrate that exposure of MDCK cells to 0.5 μM BK or 10 μM ATP elicited Ca^{2+} oscillations. *C*, challenging MDCK cells with different concentrations of BK gave an almost flat response curve for both the percentage of oscillating cells and the oscillation frequency. *D*, the concentration dependence of ATP-induced oscillations was bell-shaped with a maximum at ~10 μM ATP. *E* and *F*, comparison of the initial $[Ca^{2+}]_i$ transients (AUC and amplitude) triggered by BK (0.5 μM) and ATP (10 μM) under control (1 mM extracellular Ca^{2+}) and extracellular zero Ca^{2+} (no added Ca^{2+} + 1 mM EGTA) conditions. *A.U.*, arbitrary units. *G*, ATP and BK transients were triggered in zero Ca^{2+} medium after which Ca^{2+} (1 mM) was reintroduced to the bathing medium. SOCE (AUC) triggered in this manner was significantly larger for BK compared with ATP. *H* and *I*, example traces illustrate the effect of photolytically releasing $InsP_3$ (indicated by the *star*) on Ca^{2+} oscillations induced by BK (0.5 μM) or ATP (10 μM). *J* and *K*, the *bar chart* summarizes the percentage of cells displaying delayed or accelerated spiking activity following photorelease of $InsP_3$.

depicted in Fig. 1*D*) and 0.5 μM BK (relative location within the range of concentrations tested comparable with ATP) for further analysis of the differences between the oscillations triggered by these two agonists. We first determined whether the amplitude of the initial $[Ca^{2+}]_i$ transient triggered by BK (0.5 μM) or ATP (10 μM) was different but found they were very similar (650 ± 59 and 783 ± 110 nM, respectively, $n = 8$, $p > 0.05$) which suggests that the intracellular $InsP_3$ elevation is comparable with the two stimuli. Yet the area under the curve (AUC) for both triggers differed markedly with BK exhibiting a much larger AUC compared with ATP (Fig. 1, *E* and *F*). Because the amplitudes were not different, it follows that the BK-triggered $[Ca^{2+}]_i$ transient is longer than the one triggered by ATP (see example traces in Fig. 1*A*). The longer duration of the BK-induced $[Ca^{2+}]_i$ transient is likely to be related to Ca^{2+} entry from the extracellular space. In line with this, withdrawal of extracellular Ca^{2+} (zero extracellular Ca^{2+}) did not much affect the initial $[Ca^{2+}]_i$ transient elicited by ATP, whereas it largely reduced the one triggered by BK (Fig. 1, *E* and *F*). Further probing of SOCE by reintroducing extracellular Ca^{2+} after the $[Ca^{2+}]_i$ transient in zero extracellular Ca^{2+} conditions showed that SOCE was much larger for BK than for ATP (Fig. 1*G*).

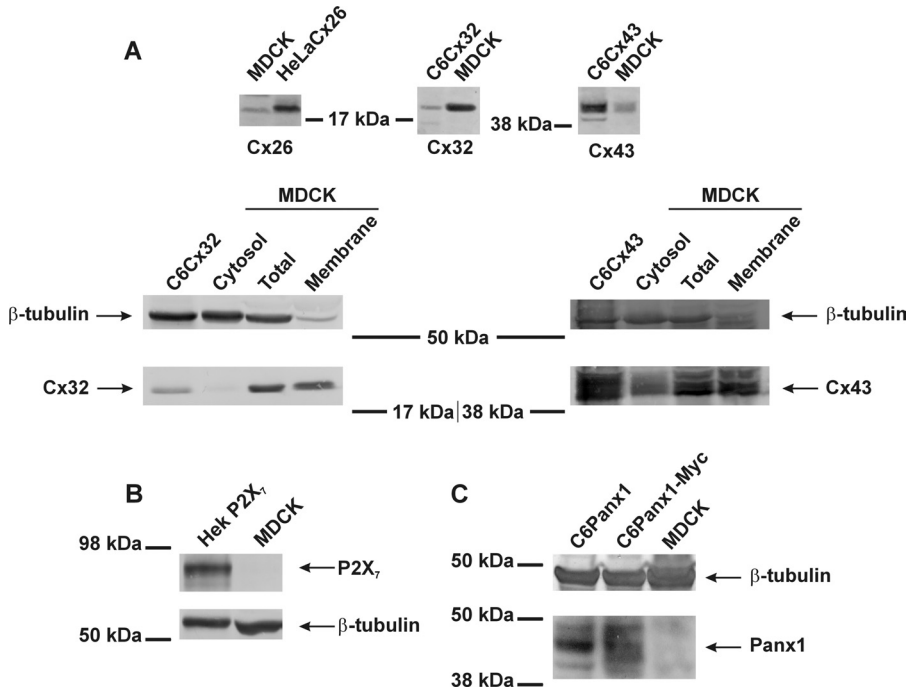

FIGURE 2. **Connexin, pannexin, and $P2X_7$ expression in MDCK cells.** *A*, Western blot analysis shows expression of Cx32 and Cx43, with a small background of Cx26. Cx32 and Cx43 were mainly present in membrane fractions, whereas their presence in the cytosol fraction was much lower. C6Cx32, C6Cx43, or HeLaCx26 were used as positive controls, and β-tubulin was a loading control. *B*, MDCK cells do not express the purinoceptor $P2X_7$. HEK cells stably transfected with $P2X_7$ were used as a positive control. *C*, Panx1 is not expressed in MDCK cells. C6 cells stably transfected with Panx1 or Panx1-Myc are used as positive controls.

Sneyd *et al.* (45) described a method to distinguish between oscillations characterized by a constant level of intracellular $InsP_3$ and those associated with oscillatory $InsP_3$ fluctuations by recording the response to an applied $InsP_3$-concentration step. If $InsP_3$ fluctuates during the Ca^{2+} oscillations, induction of a sudden $InsP_3$ increase will introduce a delay to the next Ca^{2+} spike. The delay is caused by the fact that $InsP_3$ has to recover to a level that is again compatible with Ca^{2+} oscillations; thereafter, the oscillation frequency stabilizes again. If $InsP_3$ is constant during the Ca^{2+} oscillations, an induced $InsP_3$ elevation will temporarily increase the oscillation frequency, giving accelerated oscillations (45, 46). We performed $InsP_3$ elevation experiments with flash photolysis of caged $InsP_3$ and found that the majority of the cells (~48%) showed a delayed response for both BK- and ATP-induced oscillations (Fig. 1, *H–K*). A smaller fraction of the cells displayed an accelerated response: ~10% for BK and ~22% for ATP oscillations. In the remainder of the cells $InsP_3$ elevation had no effect. These data indicate that oscillations triggered by BK and ATP are similar, at least with respect to the occurrence of $InsP_3$ oscillations.

Connexin Channel Blockers Inhibit BK-induced Ca^{2+} Oscillations but Not Those Triggered by ATP—SDS-PAGE and Western blot analysis revealed the presence of Cx32 and Cx43 in MDCK cells, with a small background expression of Cx26. Both Cx32 and Cx43 were present in the plasma membrane, whereas their presence in the cytosolic fraction was limited (Fig. 2*A*). MDCK cells did not express Panx1 or $P2X_7$, which is linked to Panx1 channels (47) (Fig. 2, *B* and *C*). When BK-triggered oscillations were elicited in the presence of the general connexin channel blocker Cbx (25 μM, 30-min preincubation and present during the 10-min observation window), the initial Ca^{2+} spike remained, but the subsequent oscillations disappeared. We further applied two peptide connexin channel inhibitors, ^{32}Gap27 and ^{43}Gap26, that target Cx32 and Cx43 channels, respectively (36, 48). Application of ^{32}Gap27/^{43}Gap26 ("Gap," 200 μM, 30-min preincubation and present during the recording) also inhibited the Ca^{2+} oscillations without perturbing the initial peak (Fig. 3*A*). ^{32}Gap27 and ^{43}Gap26, either separately or in an equimolar mix, reduced the percentage of oscillating cells to ~1/3, and Cbx reduced it to ~1/7 (Fig. 3*B*); a similar degree of inhibition was observed for the oscillation frequency (Fig. 3*C*). Superfusion experiments showed that inhibition by ^{32}Gap27/^{43}Gap26 was rapid, within ~1 min, and that oscillations reappeared upon wash-out of the peptides (Fig. 3*D*). We next tested the effect of Gap peptides and Cbx on Ca^{2+} oscillations triggered by ATP (10 μM) and found they had no effect on the percentage of oscillating cells or the oscillation frequency (Fig. 3, *E-G*). Thus, only BK-triggered Ca^{2+} oscillations are influenced by Cbx or Gap peptides. The BK-triggered Ca^{2+} oscillations were not synchronized in neighboring cells, pointing to absence of gap junctional or other synchronizing mechanisms (49–51). The rapid block of oscillations by Gap peptides suggests an effect at the level of hemichannels, as generally longer incubations are needed to also influence gap junctions (30, 32, 34). In line with this, ^{32}Gap27/^{43}Gap26 (200 μM, 60 min) had no effect on gap junction dye coupling studied with fluorescence recovery after photobleaching (Fig. 3*H*). Knockdown of Cx43 RNA showed that suppressing Cx43 expression prevented BK-triggered Ca^{2+} oscillations, in line with inhibition of oscillations by ^{43}Gap26 added alone (without ^{32}Gap27). Western blot analysis indicated a ~50% reduction of Cx43

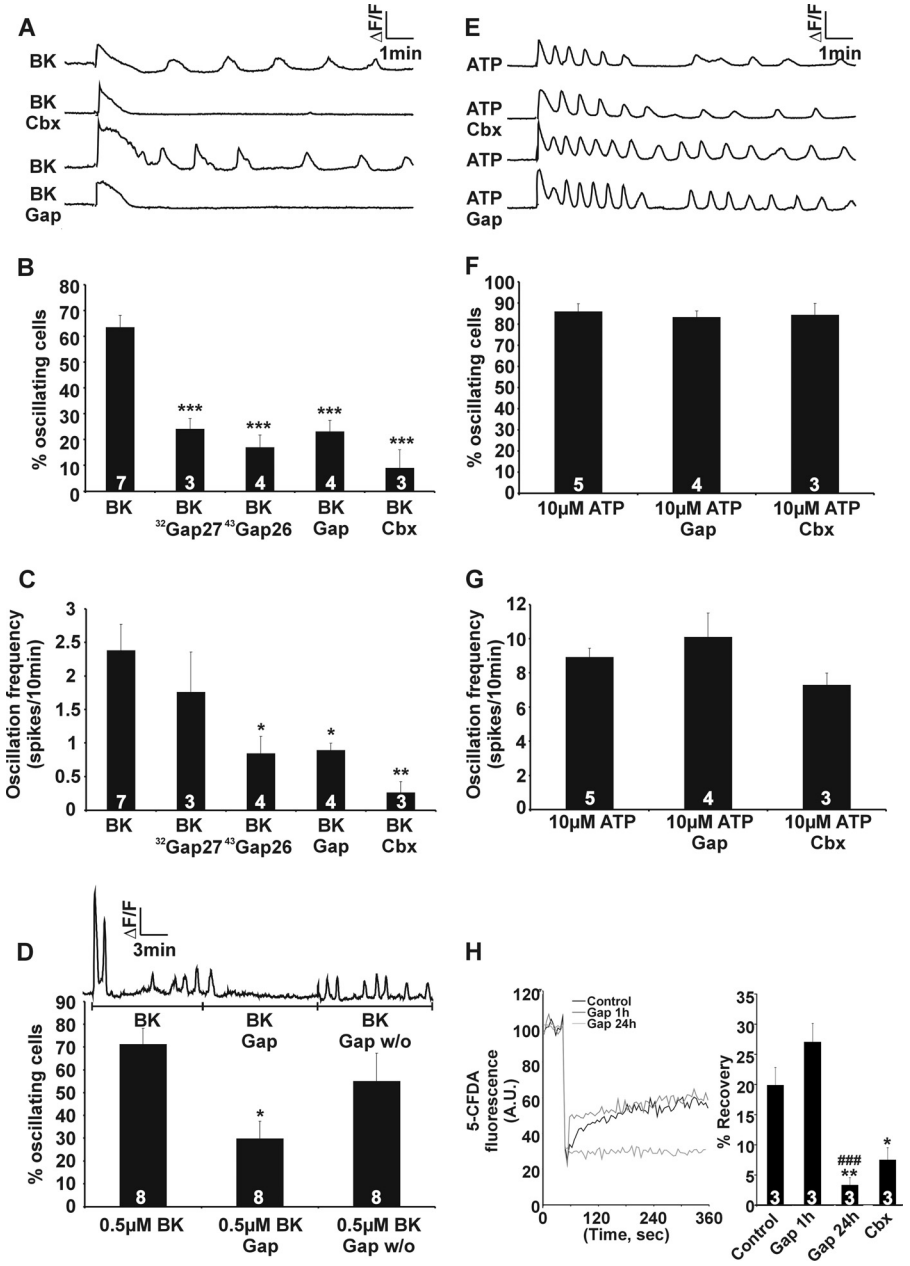

FIGURE 3. **Gap peptides and Cbx block BK-induced Ca^{2+} oscillations.** *A*, representative traces of $[Ca^{2+}]_i$ responses to BK application (0.5 μM) illustrating that Cbx (25 μM) and ^{32}Gap27/^{43}Gap26 (Gap, 200 μM) inhibit the oscillations. *B*, effect of Cbx and Gap peptides on the percentage of oscillating cells. *C*, effect of Cbx and Gap peptides on oscillation frequency. *D*, superfusion experiment illustrating that BK-triggered oscillations almost immediately disappeared after the addition of the Gap peptides. Summary data of experiments are shown below. *Stars* indicate significance compared with BK alone. *E*, example traces of Ca^{2+} responses triggered by ATP (10 μM) illustrate the absence of any effect of Cbx and Gap on the oscillations. *F*, the percentage of cells displaying oscillations in response to ATP was not altered by Cbx and Gap. *G*, the oscillation frequency with ATP stimulation was not significantly altered by Cbx and Gap. *H*, Gap junctional dye coupling was unaffected when ^{32}Gap27/^{43}Gap26 (Gap) were incubated for 1 h but strongly declined when these peptides were present for 24 h or when the aspecific connexin channel blocker Cbx (25 μM, 15 min) was used.

expression in cells transfected with SiCx43–1 (125 nM, 48 h) (Fig. 4*A*), and the number of oscillating cells in the presence of BK was reduced to a similar extent (Fig. 4, *B* and *C*). SiCx43–2 was less efficient and gave proportionally less inhibition (Fig. 4, *A* and *C*). Importantly, neither SiCx43–1 nor SiCx43–2 reduced Cx32 expression (data not shown); therefore, the oscillations that remain after Cx43 silencing may result from incomplete Cx43 knockdown or from the contribution of Cx32 hemichannels. Cx43-gene silencing did not influence ATP-triggered Ca^{2+} oscillations (Fig. 4, *D* and *E*).

Lowering Extracellular Ca^{2+} Differentially Affects BK- and ATP-induced Oscillations—Hemichannels may contribute to the oscillations via ATP release acting in an autocrine manner (28, 34) or via Ca^{2+} entry (29). We first set out to find evidence for hemichannel opening in response to BK. Exposure of cells preloaded with calcein (a hemichannel-permeable fluorescent dye with a molecular mass of 623 Da (43)) to BK (0.5 μM) increased the calcein efflux rate, and this effect was counteracted by ^{32}Gap27/^{43}Gap26 (Fig. 5*A*). In contrast, ATP (10 μM) did not accelerate dye efflux (Fig. 5*A*). BK-triggered calcein

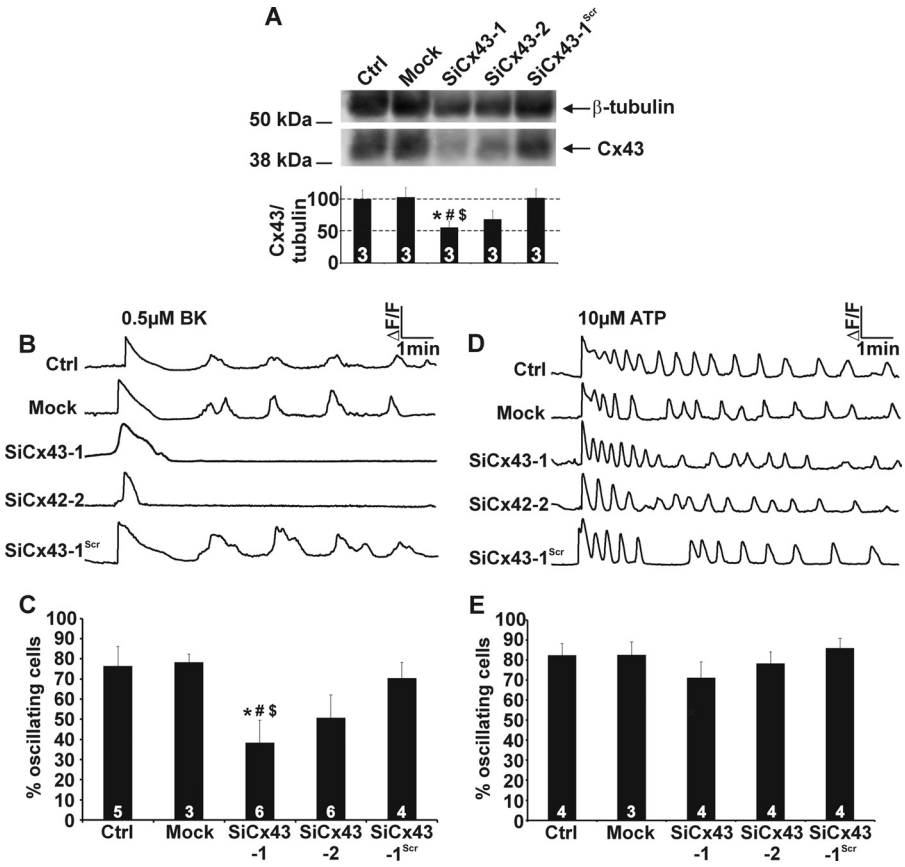

FIGURE 4. **Effect of Cx43 gene silencing on Ca^{2+} oscillations.** *A*, silencing of Cx43 gene expression in MDCK cells demonstrates significantly reduced expression to ~50% of the control signals (the *star* compares to Ctrl, the *number sign* compares to Mock-treated cultures, and the *dollar sign* compares to cells transfected with a scrambled sequence). *B*, example traces of Ca^{2+} responses triggered by BK (0.5 μM) for the different treatment conditions shown in *panel A*. *C*, Cx43 knockdown in MDCK cells approximately halved the number of oscillating cells in the presence of 0.5 μM BK (significance signs as in *panel A*). *D* and *E*, Cx43 gene silencing did not influence Ca^{2+} oscillations triggered by 10 μM ATP.

release could be furthermore reduced by buffering increases in $[Ca^{2+}]_i$ using the Ca^{2+} chelator BAPTA-AM (Fig. 5*B*). Phospholipase A_2 is reported to be activated by BK (52, 53) and is involved in connexin hemichannel opening (36); however, phospholipase A_2 inhibition by arachidonyl trifluoromethyl ketone had no effect on the percentage of cells displaying oscillations in response to BK (63 ± 7% oscillating cells in control *versus* 65 ± 7% oscillating cells in arachidonyl trifluoromethyl ketone-treated cells, $n = 4$), further emphasizing that $[Ca^{2+}]_i$ changes are necessary for hemichannel opening. We next tested whether ATP release through open hemichannels played a role in BK-induced Ca^{2+} oscillations. We applied apyrase VI/VII (to degrade extracellular ATP), PPADS, or suramin (to inhibit purinergic P2 receptors), and 8-(*p*-sulfophenyl)theophylline (to inhibit adenosine $A1/A2_B$ receptors), but these agents did not significantly influence the percentage of oscillating cells or the oscillation frequency (Fig. 5, *C* and *D*). We recently reported that ATP release via hemichannels was involved in BK-induced oscillations in RBE4 brain endothelial cells (34), and we speculated that MDCK cells display a stronger ectonucleotidase activity than RBE4 cells. In line with this, we found that ATP added to the incubation solution above the cells was more rapidly degraded in MDCK cells as compared with RBE4 cell cultures (Fig. 5, *E* and *F*), indicating stronger ectonucleotidase activity in MDCK cells. Thus, ATP released via BK-induced hemichannel opening likely has no downstream effects on purinergic receptors or Ca^{2+} oscillations in MDCK cells due to its rapid degradation.

Because ATP release does not contribute to BK-triggered Ca^{2+} oscillations in MDCK cells, we evaluated the role of Ca^{2+} entry through hemichannels. To this purpose we decreased the driving force for Ca^{2+} entry by lowering the extracellular Ca^{2+} concentration. The latter may result in hemichannel opening (54–56), compromising the interpretation of the intended experiments. However, concentrations below ~0.2 mM are reported to open hemichannels (57); thus, we applied 0.5 mM instead of the normal extracellular Ca^{2+} concentration of 1 mM. Calcein release experiments confirmed that exposure of MDCK cells to 0.5 mM extracellular Ca^{2+} did not trigger hemichannel opening, whereas a further reduction of extracellular Ca^{2+} to 0.2 mM or the subnanomolar range indeed provoked the opening of hemichannels (Fig. 6, *A* and *B*). Application of 0.5 mM extracellular Ca^{2+} during BK exposure interrupted the Ca^{2+} oscillations, and re-addition of normal extracellular Ca^{2+} restored the oscillations (Fig. 6*C*). The number of oscillating cells was strongly reduced by 0.5 mM extracellular Ca^{2+} (Fig. 6*D*). Interestingly, Ca^{2+} oscillations induced by ATP decreased in amplitude but were not suppressed by switching to 0.5 mM extracellular Ca^{2+}, and the percentage of oscillating cells was not significantly altered (Fig. 6, *E* and *F*). Thus, BK-induced

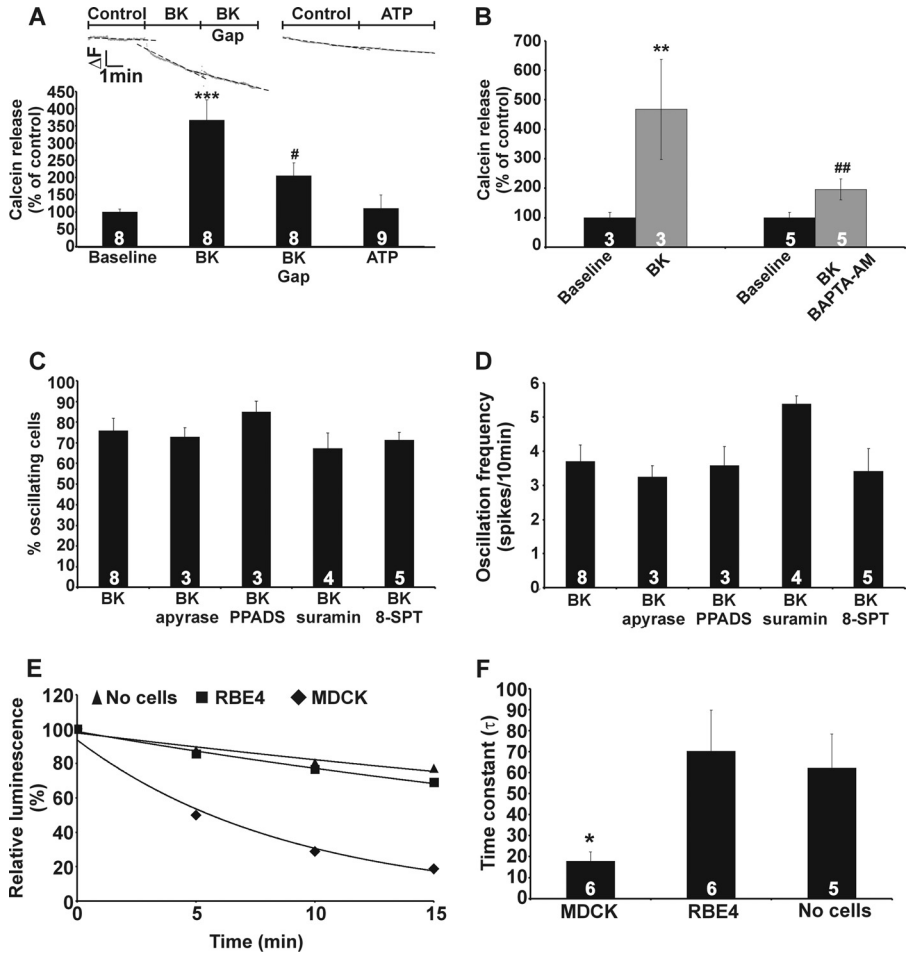

FIGURE 5. **Calcein hemichannel studies and involvement of ATP release.** *A*, BK (0.5 μM) stimulated the rate of calcein release from MDCK cells, and this was rapidly inhibited by ^{32}Gap27/^{43}Gap26 (Gap, 200 μM). ATP did not influence the rate of calcein release. *B*, BK-triggered calcein release was inhibited by $[Ca^{2+}]_i$ chelation with BAPTA-AM (5 μM, 1 h preincubation). *Asterisks* indicate significance compared with baseline, and *number signs* indicate a significant difference compared with BK-triggered calcein release. *C* and *D*, apyrase (5 units/ml, 30 min preincubation), PPADS (75 μM, 30 min preincubation), suramin (200 μM, 30 min preincubation), or 8-(*p*-sulfophenyl)theophylline (*8-SPT*, 100 μM, 30 min preincubation) did not significantly influence BK-induced Ca^{2+} oscillations. *E*, example traces illustrate the spontaneous decrease of ATP concentration after the addition of exogenous ATP to the medium above the cells. In MDCK cells, ATP decreased much more rapidly compared with rat brain endothelial cells (RBE4) or no cells being present. *F*, a *bar chart* summarizes analysis of experiments shown in *E*. The data indicate prominent ectonucleotidase activity in MDCK cells.

oscillations are dependent on extracellular Ca^{2+}, indicating a contribution of SOCE or Ca^{2+} entry via hemichannels to the oscillation mechanism. Importantly, hemichannels did not contribute to SOCE, as ^{32}Gap27/^{43}Gap26, added during reintroduction of extracellular Ca^{2+} in an experiment as shown in Fig. 1*G*, did not influence SOCE after BK stimulation (data not shown).

ATP-induced Ca^{2+} Oscillations Are Inhibited by CytC, whereas BK-induced Oscillations Are Inhibited by Both CytC and Cx43-targeting CT9 Peptide—A critical and essential factor in the generation of Ca^{2+} oscillations is the presence of positive and negative feedback actions (11, 12, 15). In the classical scheme of $InsP_3$-triggered Ca^{2+} oscillations, this feedback acts at $InsP_3$Rs, with low $[Ca^{2+}]_i$ stimulating ER Ca^{2+} release and higher concentrations being inhibitory (7) (Fig. 7*B*). Based on dye uptake and ATP release studies, hemichannels composed of Cx32 and Cx43 have also been demonstrated to display a bell-shaped $[Ca^{2+}]_i$ dependence for opening (35, 36) (Fig. 7*D*). There is an interesting set of tools available to influence the bell-shaped Ca^{2+} dependence of $InsP_3$Rs and hemichannels. Negative feedback of Ca^{2+} on $InsP_3$Rs can be alleviated by CytC (58) (Fig. 7, *A* and *B*). In fact, this is an important mechanism contributing to apoptotic cell death because CytC binding to the $InsP_3$ receptor removes the brake on ER Ca^{2+} release, resulting in Ca^{2+} accumulation in mitochondria that amplifies CytC release in a vicious circle (59–61). Inhibiting the declining phase of $InsP_3$R activity is expected to disrupt oscillations because of the essential role of negative feedback as an OFF signal in the oscillation cycle. We recently reported that a synthetic peptide composed of the last 10 amino acids of the C-terminal (CT) tail of Cx43 prevented the inhibitory phase of the bell-shaped $[Ca^{2+}]_i$ dependence of hemichannel opening (37) (Fig. 7, *C* and *D*). If this bell-shaped $[Ca^{2+}]_i$ dependence contributes as a hemichannel-related mechanism in the oscillations, it is expected (similar as for the $InsP_3$R) that such CT peptide would inhibit the oscillations by removing the OFF signal. We used CytC and CT9 peptide (last nine amino acids of the Cx43 CT) to selectively interfere with the negative feedback of Ca^{2+} on $InsP_3$Rs and connexin hemichannels, respectively, and examined their effect on the BK-induced Ca^{2+} oscillations.

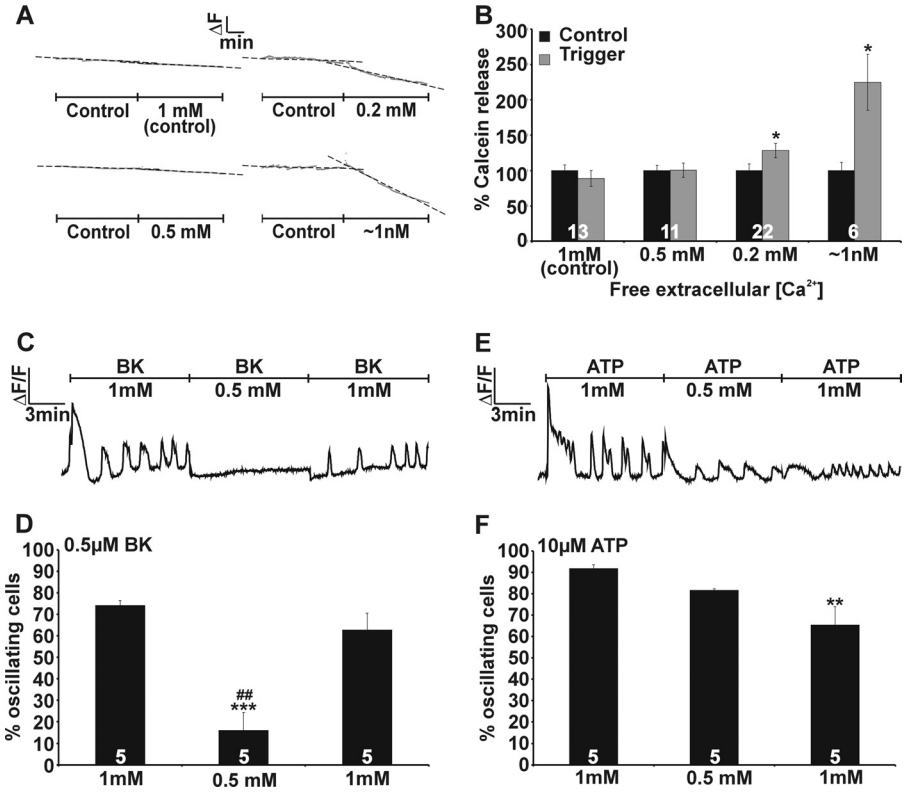

FIGURE 6. **Depletion of extracellular Ca^{2+} inhibits BK-induced Ca^{2+} oscillations.** *A*, applying 0.5 mM Ca^{2+} solution did not trigger calcein release in MDCK cells, whereas 0.2 mM or ~1 nM free extracellular Ca^{2+} solutions did. *B*, the *bar chart* summarizes the effect of low extracellular Ca^{2+} on calcein release. The *asterisk* indicates a significant difference from the corresponding control. *C*, switching to 0.5 mM extracellular Ca^{2+} during BK-induced Ca^{2+} oscillations immediately interrupted the oscillations, and the effect was reversible upon switching to normal extracellular Ca^{2+}. *D*, low extracellular Ca^{2+} (0.5 mM) strongly reduced the number of oscillating cells. *E* and *F*, low extracellular Ca^{2+} (0.5 mM) had no effect on ATP-induced oscillations. *, significantly different from 0.5 μM BK before Ca^{2+} depletion; # significantly different from oscillations after restoration of extracellular Ca^{2+}.

CytC binds to $InsP_3R$ type 1 and 3 (58), which are both present in MDCK cells (62). CT9 and CytC are plasma membrane-impermeable, and we used *in situ* electroporation to load these substances into the cells without disturbing cell function or viability (41, 42). To identify the cells loaded with these agents, we included the fluorescent markers DTR/dextran fluorescein and PI that have molecular masses in the range of CytC (~12 kDa) and CT9 (~1 kDa), respectively. Electroporation loading allows analysis of the Ca^{2+} oscillations in loaded as well as non-loaded (control) cells (Fig. 8, *A* and *F*). After applying BK (0.5 μM), cells loaded with CytC (~1 μM intracellular concentration) displayed significantly less oscillatory activity as compared with control cells in the same culture and as compared with cells loaded with vehicle-only (Fig. 8, *B* and *C*). The decreased oscillations were not caused by apoptosis (triggered by CytC), as CytC exposure was short (10 min), and annexin V staining to detect early apoptotic cells was negative (data not shown). We further applied the IP_3RCYT peptide that corresponds to the CytC binding residues of the $InsP_3R1$ (located on the C terminus), thereby preventing the binding of CytC to $InsP_3R$ (38, 63). Inclusion of the IP_3RCYT peptide (~5 μM intracellular concentration) prevented the CytC-mediated decrease in percentage of cells displaying Ca^{2+} oscillations (Fig. 8*C*). To further document the involvement of $InsP_3$ signaling in BK-triggered oscillations, we tested inhibition of PLC with U73122, inhibition of $InsP_3Rs$ with xestospongin C (*XeC*), and pre-emptying of thapsigargin-sensitive Ca^{2+} stores; all these conditions suppressed BK-triggered oscillations, as expected (Fig. 8*E*). Loading cells with CytC did not affect the AUC (Fig. 8*D*) or peak amplitude (not shown) of the initial $[Ca^{2+}]_i$ transient triggered by BK under zero extracellular Ca^{2+} conditions, indicating no effect of CytC on the Ca^{2+} dynamics associated with the initial $[Ca^{2+}]_i$ transient triggered by BK. However, the addition of thapsigargin after BK stimulation (still under zero extracellular Ca^{2+} conditions) released less Ca^{2+} from CytC-loaded cells than from control cells (Fig. 8*D*). Hence, Ca^{2+} store emptying was more complete with CytC, and this substance thus potentiates BK-triggered ER Ca^{2+} release. This effect of CytC is in line with its expected action as a stimulator of $InsP_3Rs$, which is the result of a decreased $InsP_3R$ inhibition by high $[Ca^{2+}]_i$ (38). Because CytC did not influence the amplitude of the $[Ca^{2+}]_i$ transient, we anticipated that the larger ER Ca^{2+} release flux was more effectively taken up by mitochondria. Accordingly, we found that the mitochondrial Ca^{2+} response (measured with RhodFF) after BK stimulation was larger in CytC-loaded cells as compared with control (Fig. 8*D*).

When cells were loaded with the Cx43-targeting CT9 peptide (last 9 amino acids of the Cx43 CT; ~100 μM intracellular concentration), BK-induced oscillations were significantly inhibited compared with non-loaded control cells in the same culture and to cells loaded with vehicle-only (Fig. 8, *G* and *H*). By contrast, $CT9^{Rev}$ peptide (reversed sequence) did not affect the number of oscillating cells (Fig. 8*H*). The last isoleucine residue of Cx43 is essential for interaction with the scaffolding

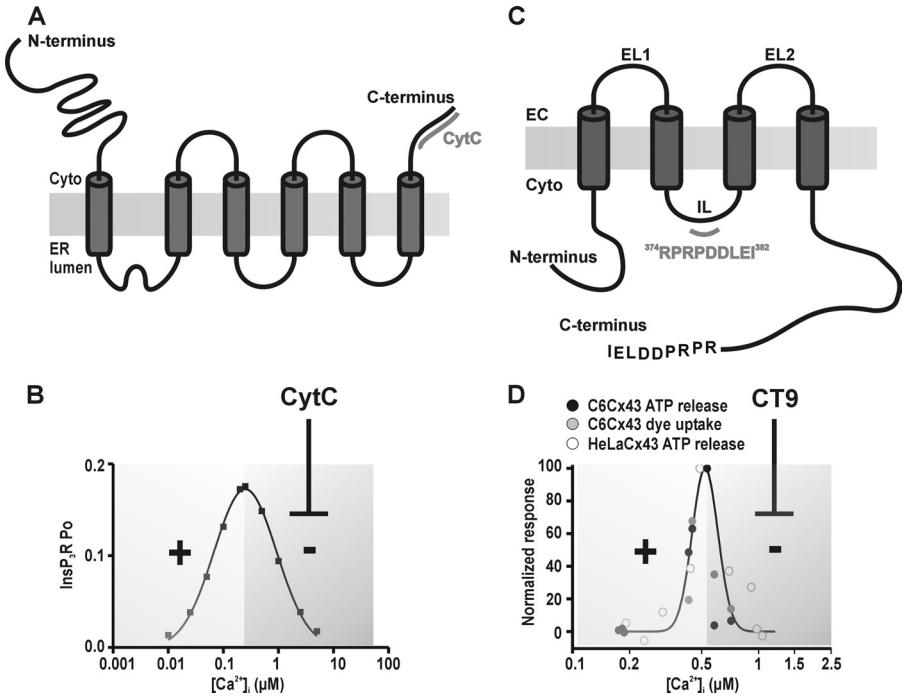

FIGURE 7. **CytC and CT9 influence $InsP_3Rs$ and connexin hemichannels, respectively.** *A*, CytC binds to the C-terminal domain of $InsP_3R$. *B*, $InsP_3Rs$ have a bell-shaped $[Ca^{2+}]_i$ dependence of the open probability (*Po*) with below 250 nM concentrations potentiating $InsP_3R$ opening and higher concentrations acting inhibitory. The bell-shaped dose response curve is derived from parameters and equations described in Ref. 97 for $InsP_3R$ type 1. CytC binds to $InsP_3R$ and removes the inhibitory effects of high $[Ca^{2+}]_i$ on $InsP_3R$ open probability. *C*, CT9 peptide is composed of the last 9 amino acids of the Cx43 C terminus and interacts with a sequence on the intracellular loop (*IL*). *EC*, extracellular. *D*, Ca^{2+} activation of hemichannels composed of Cx43 are characterized by a bell-shaped $[Ca^{2+}]_i$ dependence (hemichannel ATP release and dye uptake studies, derived from data in Ref. 36). CT9 peptide removes the declining phase at $[Ca^{2+}]_i$ above 500 nM (37).

protein ZO-1 (64), and CT9 peptide is thus expected to bind to ZO-1 and prevent Cx43/ZO-1 binding (37, 65). To investigate whether Ca^{2+} oscillations are suppressed by dissociation of the Cx43/ZO-1 complex, we used a peptide similar to CT9 that is lacking the last isoleucine residue (CT9ΔI). This peptide does not disrupt Cx43/ZO-1 interaction (37) but was equally potent in inhibiting BK-triggered Ca^{2+} oscillations (Fig. 8*H*). Therefore, the CT9-induced block of Ca^{2+} oscillations is not likely caused by altering Cx43/ZO-1 interactions. As observed for CytC, the AUC or peak amplitude of the first $[Ca^{2+}]_i$ increase was not influenced by CT9 or CT9ΔI, indicating that the $InsP_3$ production and initial $InsP_3R$ responses were not affected by these treatments. In addition, baseline $[Ca^{2+}]_i$ was not affected by CytC or CT9: 58 ± 5 nM for CytC and 56 ± 4 nM for CT9 compared with 57 ± 5 nM for control ($n = 4$). Calcein release was not different in CT9- or CytC-loaded cells from their controls outside the loading zone (88 ± 8 and 107 ± 31%, respectively, *versus* 100% in control, $n = 3$), indicating that CT9 and CytC by themselves do not trigger hemichannel opening.

Recently, O'Quinn *et al.* (66) showed that the CT9 peptide triggers a PKC-mediated phosphorylation of the Cx43 Ser-368 consensus site in cardiomyocytes, but we could not observe such an effect when MDCK cells were treated with cell-permeable Tat-CT9 peptide (Fig. 8*I*).

We next tested CytC and CT9 peptide on Ca^{2+} oscillations elicited by ATP (Fig. 9) and found that CytC was inhibitory and inclusion of the IP_3RCYT peptide removed this inhibition. Again, Ca^{2+} store emptying was more complete, and mitochondrial Ca^{2+} response was larger with CytC (Fig. 9*C*). Also, inhibition of PLC and $InsP_3R$ as well as pre-emptying of thapsigargin-sensitive Ca^{2+} stores suppressed oscillatory activity (Fig. 9*F*). Importantly, CT9 peptide had no effect on ATP-induced Ca^{2+} oscillations. These experiments indicate that ATP-induced oscillations rely on $InsP_3Rs$, whereas those induced by BK rely on both $InsP_3Rs$ and hemichannels.

We further tested whether hemichannels were sufficient as a mechanism to obtain oscillations without a contribution of $InsP_3Rs$. Hemichannel opening can be triggered by $[Ca^{2+}]_i$ elevation without increasing $InsP_3$ and thus without activating $InsP_3Rs$ and $InsP_3R$-based oscillations. $[Ca^{2+}]_i$ elevation triggered by photolytic release of Ca^{2+} did not trigger Ca^{2+} oscillations ($n = 4$), indicating that hemichannels are not sufficient as an oscillatory mechanism and $InsP_3Rs$ are the dominant mechanism leading to oscillations.

DISCUSSION

The present data demonstrate that BK- and ATP-induced Ca^{2+} oscillations display distinct properties in MDCK cells. Oscillations induced by BK (i) showed a flat concentration dependence of frequency and percentage of responding cells, (ii) were inhibited by Cbx, Gap peptides, and Cx43 gene silencing, (iii) disappeared when extracellular Ca^{2+} was lowered, and (iv) were inhibited by CytC and CT9 peptide. By contrast, ATP-induced oscillations (i) showed a bell-shaped ATP concentration dependence, (ii) were not influenced by Cbx, Gap peptides, or Cx43 silencing, (iii) were not abolished by lowering extracellular Ca^{2+}, and (iv) were inhibited by CytC but not by CT9

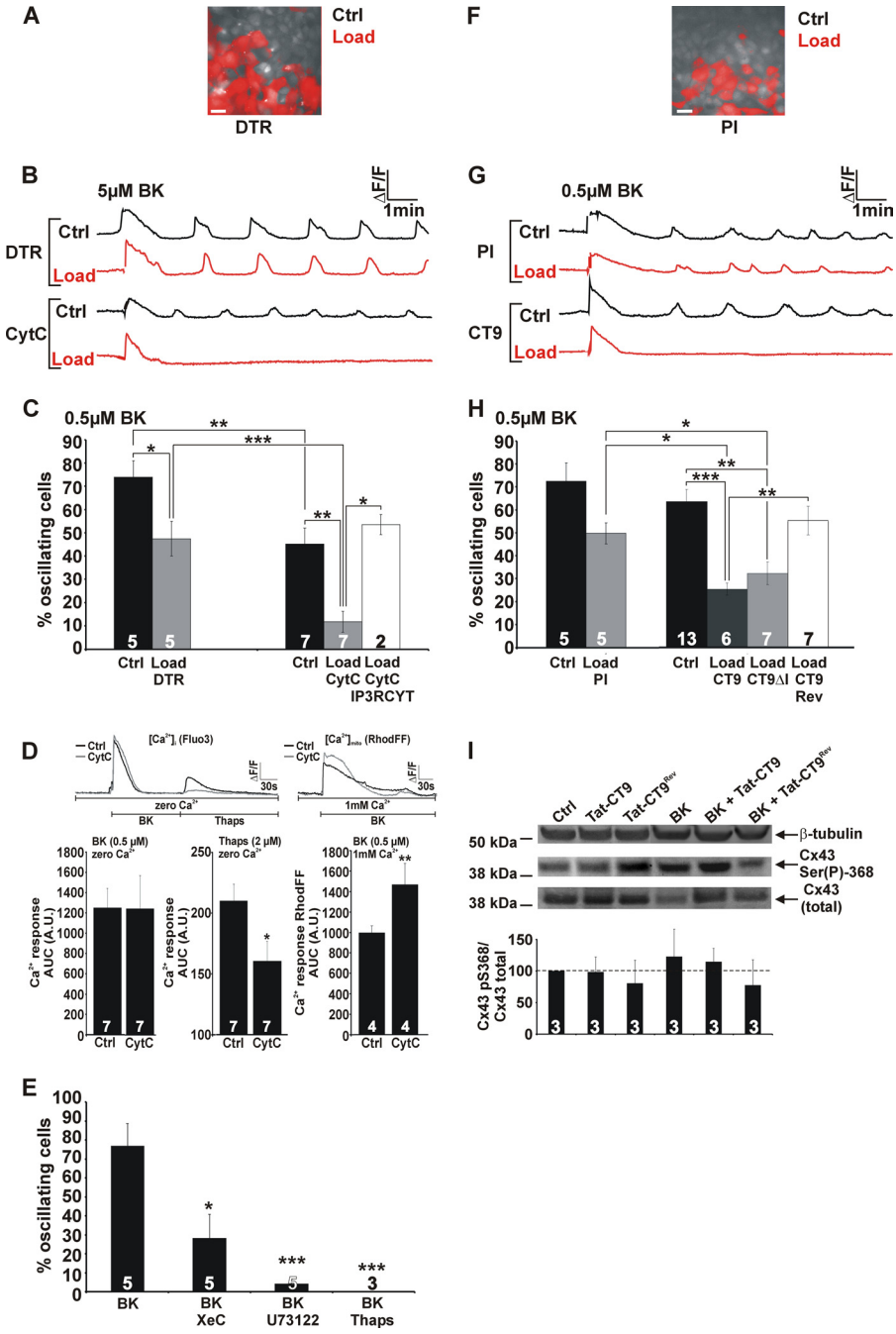

FIGURE 8. **CytC and CT9 inhibit BK-induced Ca^{2+} oscillations.** *A*, cells were loaded with CytC or with vehicle only (DTR) by *in situ* electroporation. Loaded cells are in *red* (*Load*), and non-loaded cells are gray (*Ctrl*). The *scale bar* is 25 μm. *B*, representative traces of CytC loaded cells (*Load*) and control cells (*Ctrl*). Parallel experiments were done with the cells loaded with vehicle only (*DTR*). *C*, average data of experiments as illustrated in the previous panel. The loading procedure resulted by itself in some suppressive effect on the oscillations (percentage of oscillating cells). CytC strongly reduced the oscillations and co-loading together with IP_3RCYT peptide removed the inhibitory effect of CytC. The *stars* indicate a significant difference between the bars indicated. *D*, CytC did not affect the initial $[Ca^{2+}]_i$ transient triggered by 0.5 μM BK (2 min in zero Ca^{2+} medium). Subsequent addition of thapsigargin (2 μM, 3 min, in zero Ca^{2+} medium) liberated less Ca^{2+} from intracellular stores in CytC-loaded cells compared with their controls, indicating more complete store emptying. Mitochondrial Ca^{2+} uptake was larger in cells containing CytC (mitochondrial Ca^{2+} concentration, $[Ca^{2+}]_{mito}$, was measured with RhodFF). *E*, pretreatment with Xestospongin-C (*XeC*; 10 μM, 1 h), U73122 (10 μM, 1 h), and thapsigargin (*Thaps*; 2 μM, 10 min) reduced the number of oscillating cells triggered by BK. *F*, cells were loaded with CT9 or with vehicle only (*PI*, similar to *panel A*). *G*, representative traces of loaded and control cells. *H*, CT9 peptide and CT9ΔI peptide significantly reduced the percentage of oscillating cells, in contrast to $CT9^{Rev}$. Significant differences are indicated as explained in *panel C*. *I*, Western blot analysis for Cx43-specific phosphorylated Ser-368 and total levels of Cx43 in control cells and cells treated with Tat-CT or Tat-CT^{Rev} (100 μM, 30 min) in the presence or absence of BK (0.5 μM). β-Tubulin was used as a loading control. The *bar chart* summarizes data derived from different Western blots.

peptide. Some data point to the involvement of hemichannels: (i) BK potentiated calcein dye release, whereas ATP did not, (ii) BK-triggered calcein release was rapidly (~1 min) inhibited by Gap peptides, whereas 60 min of incubation with these peptides had no effect on dye coupling, and (iii) BK-induced Ca^{2+} oscillations were inhibited by CT9 peptide that removes the Ca^{2+} inhibition of Cx43 hemichannels but not by $CT9^{rev}$ peptide. The fact that the oscillations were not synchronized between

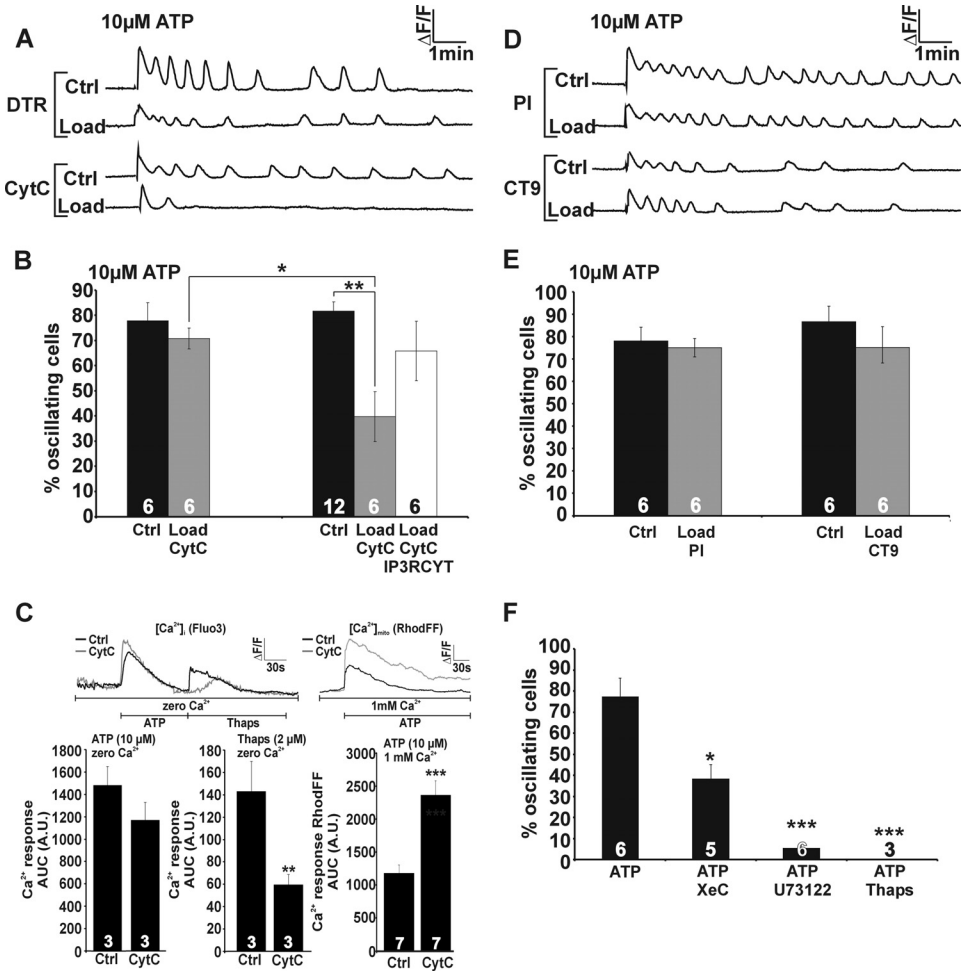

FIGURE 9. **ATP-induced Ca^{2+} oscillations are inhibited by CytC but not by CT9 peptide.** Experiments as in Fig. 8 but now performed with ATP as the oscillation-inducing stimulus. *A*, example traces of vehicle/CytC-loaded cells and their controls. *B*, CytC inhibited the oscillatory activity, and this effect was suppressed by co-loading with IP_3RCYT peptide. *C*, less Ca^{2+} was liberated from intracellular stores in the presence of CytC, indicating more complete store emptying; accordingly, mitochondrial Ca^{2+} uptake was larger. *D*, representative traces of vehicle/CT9-loaded cells. *E*, CT9 peptide had no effect on ATP-triggered oscillations. *F*, Xestospongin-C, U73122, and thapsigargin inhibited ATP-triggered oscillations. Significance symbols are as defined in Fig. 8.

cells furthermore argues against a contribution of gap junctions.

ATP-induced Ca^{2+} oscillations displayed a bell-shaped concentration dependence. An S-shaped concentration dependence is more typical (13, 67–69), but it is well known that oscillations can only occur in a limited range of $InsP_3$ concentrations so the disappearance of the oscillations at high ATP concentration may well result from too high an intracellular $InsP_3$ level (45, 70, 71). BK-induced oscillations had a flat concentration dependence, a finding also reported by others (72–74). Despite the importance of encoding the strength of agonist stimulation in the frequency of oscillations, it is not uncommon that spiking frequencies are independent of agonist concentration. According to the dynamic desensitization mechanism that occurs upon stimulation of mGluR5 (75) or the M_3 muscarinic receptor (76), elevated levels of $[Ca^{2+}]_i$ and diacylglycerol activate PKC that phosphorylates and desensitizes the receptor, thereby limiting $InsP_3$ production and stabilizing the oscillation frequency. BK does activate PKC (77), and PKC phosphorylation consensus sites in BK receptors have been identified (78), but further studies are required to determine whether dynamic desensitization is involved here.

Ca^{2+} oscillations were previously found to be inhibited by octanol, palmitoleic acid, and 18αGA (28) by antibodies directed against connexins and by Gap peptides (29, 34), all known blockers of connexin channels. Conversely, stimulating hemichannel responses with the anti-arrhythmic peptide AAP (79) has been reported to induce Ca^{2+} oscillations (80). Ca^{2+} oscillations triggered by BK were inhibited by ^{32}Gap27/^{43}Gap26 peptides within 1 min, as reported by others (81), and the Gap peptides did not influence the initial $[Ca^{2+}]_i$ transient triggered by BK. The latter indicates that the $InsP_3$-triggered Ca^{2+} release was not influenced by the Gap peptides, which is in accordance with our observation that these peptides do not influence $[Ca^{2+}]_i$ transients triggered by photolytic release of $InsP_3$ (34). BK potentiated calcein dye efflux from MDCK cells, indicating hemichannel opening. This opening is likely caused by the elevation of $[Ca^{2+}]_i$ to values in the 500 nM range that are appropriate for activation of Cx32 and Cx43 hemichannels (35, 36). BK-triggered calcein efflux was rapidly inhibited by the Gap peptides, in line with previous experimental work (34) and complemented by recent single-channel electrophysiological studies that indicate Gap peptide inhibition of unitary currents through Cx43 hemichannels with a time constant in the order

of minutes.[4] The contribution of hemichannel opening to the Ca^{2+} oscillations appeared to be related to Ca^{2+} entry, as indicated by the low extracellular Ca^{2+} experiments, and was not related to hemichannel ATP release. We cannot exclude hemichannel ATP release, but our results indicate rapid ATP degradation at the surface of MDCK cells, lowering its concentration below the threshold for purinergic receptor activation. A role for hemichannels as a non-selective Ca^{2+}-entry route has been postulated under varying circumstances including alkalinization (Cx43 (82)) and metabolic inhibition (Cx32 (83) and Cx43 (84)). Ca^{2+} entry contributes to reloading of ER Ca^{2+} stores, and the entry rate can influence the interspike interval and thus the oscillation frequency (85). At low agonist concentrations, hardly any Ca^{2+} is lost from the ER (86) and Ca^{2+} entry may, under those circumstances, act to sensitize the $InsP_3R$ to produce a regenerative Ca^{2+} spike (87) or exert positive feedback on PLC-mediated $InsP_3$ production (19, 88). The present study shows that Ca^{2+} entry, related to SOCE or as a consequence of hemichannel opening (or a combination of both), is more prominent with BK than with ATP as a stimulus.

Ca^{2+}-mediated feedback actions residing at different levels of the Ca^{2+} signaling cascade (GPCR, $InsP_3R$, or PLC) lie at the basis of Ca^{2+} oscillations (10, 18–23). Ca^{2+} activation of hemichannel-dye uptake and ATP release is, like the $InsP_3R$ open probability, characterized by a bell-shaped $[Ca^{2+}]_i$ response curve (35, 36) (Fig. 7*D*), and recent evidence shows that unitary currents through Cx43 hemichannels display a similar bimodal $[Ca^{2+}]_i$ dependence.[4] This bimodal $[Ca^{2+}]_i$ dependence may introduce additional positive and negative feedback that contributes to the Ca^{2+} oscillations. Thus, we used CT9 peptide that overcomes Cx43 hemichannel inhibition at high $[Ca^{2+}]_i$ without influencing hemichannel activity at lower $[Ca^{2+}]_i$ (37). Ca^{2+}-dependent activation of hemichannels has been proposed to involve binding of the C-terminal tail to the intracellular loop of Cx43. Conversely, hemichannel inhibition at high $[Ca^{2+}]_i$ is mediated by Ca^{2+} activation of actomyosin that disrupts the loop/tail interaction. The addition of CT9 peptide will substitute for the disrupted C-terminal tail binding by interacting with the cytoplasmic loop and thereby preventing high $[Ca^{2+}]_i$ inhibition of hemichannels (37). Here, we show that CT9 but not the reversed sequence inhibits Ca^{2+} oscillations induced by BK. CT9 inhibition of BK-induced oscillations is mediated by an effect on Cx43 but not on Cx32. Unfortunately, a CT9 analog for Cx32 is not yet available. Both Cx43 and Cx32 appear to be essential in the BK-triggered Ca^{2+} oscillations, as interfering with each of these connexins individually prevented the oscillations. This is in line with the fact that hemichannels composed of Cx32 also have, like those composed of Cx43, a bell-shaped $[Ca^{2+}]_i$ dependence.

Mathematical modeling has demonstrated that positive and negative feedback on voltage-gated Ca^{2+} entry is by itself sufficient to generate Ca^{2+} oscillations (89). In contrast, the present experiments show that a forced $[Ca^{2+}]_i$ change does not induce Ca^{2+} oscillations, indicating that the Ca^{2+}-sensitive and Ca^{2+} entry-mediating hemichannels are not sufficient as an oscillation mechanism. Consistent with this is the observation that BK-triggered Ca^{2+} oscillations largely rely on $InsP_3Rs$ (Fig. 8). CytC removes $InsP_3R$ inactivation at high $[Ca^{2+}]_i$, giving increased ER Ca^{2+} release leading to a gradually increasing $[Ca^{2+}]_i$, mitochondrial Ca^{2+} overload, and apoptosis (58). We did not observe $[Ca^{2+}]_i$ elevation after CytC application, but this is probably related to the relatively short (10 min) time window used to record Ca^{2+} oscillations. Additionally, high $[Ca^{2+}]_i$ inhibition of $InsP_3Rs$ is not the only OFF mechanism mediating $[Ca^{2+}]_i$ restoration to the resting level; Ca^{2+} pumps, like sarcoplasmic/endoplasmic and plasma membrane Ca^{2+} ATPases, which are not affected by CytC (58), will ensure proper maintenance of normal $[Ca^{2+}]_i$ within the 10-min time frame of our recordings. Importantly, our data are the first demonstration in intact cells that CytC promotes ER Ca^{2+} release, supporting its proposed action as an antagonist of high $[Ca^{2+}]_i$ inhibition of $InsP_3Rs$ (38). CytC also stimulated mitochondrial Ca^{2+} uptake, but this may be a direct consequence of the increased ER Ca^{2+} release.

Interestingly, ATP-induced oscillations were also inhibited by CytC but not by CT9 peptide, indicating that these oscillations thrive exclusively on $InsP_3$-based mechanisms. Thus, BK-triggered oscillations are based on $InsP_3Rs$ with an additional hemichannel component. Because hemichannels can be activated by moderate (<500 nM) $[Ca^{2+}]_i$ elevation, we hypothesize that these channels open with each Ca^{2+} spike and contribute with Ca^{2+} entry during the rising phase. When the spike amplitude rises above 500 nM, hemichannels close again and contribute with an OFF mechanism that adds to the OFF mechanism of $InsP_3R$ channels. The fact that hemichannels are by themselves not sufficient to mediate oscillations probably results from a slower kinetics for opening than for closing. Previous work has indeed suggested that hemichannel activation by Ca^{2+} is characterized by several intermediate signaling steps pointing to slow activation kinetics (36). A point of notice is that the duration of the primary Ca^{2+} peak was different for both triggers: ~40 s for 0.5 μM BK and 15 s for 10 μM ATP (see example traces in Fig. 1). Preliminary modeling using the activation kinetics of hemichannel opening presented in Refs. 35 and 36 indeed indicates that a $[Ca^{2+}]_i$ rise of 40 s (BK) can trigger the opening of twice as much hemichannels compared with a peak that lasts only 15 s (ATP). Additionally, the Ca^{2+} spikes of BK-triggered oscillations were generally of longer duration than those triggered by ATP (see example traces in Fig. 1) making it possible that these Ca^{2+} transients were more efficient in inducing hemichannel opening. We speculate that the more prominent contribution of SOCE with BK stimulation is more effective in triggering hemichannel opening because it occurs more localized and in close proximity of the hemichannels in the plasma membrane.

Our experiments indicate that hemichannels actively contribute to BK-induced Ca^{2+} oscillations by providing a Ca^{2+} entry pathway characterized by a bimodal $[Ca^{2+}]_i$ dependence. This contribution is crucial as inhibition of this pathway blocks the oscillations. Several compounds like the $InsP_3R$ inhibitor 2-APB used to explore the mechanism of Ca^{2+} oscillations (90) are known to inhibit connexin hemichannels (91). Additionally, the non-selective Ca^{2+} channel blocker La^{3+} has frequently

[4] N. Wang and L. Leybaert, unpublished observation.

been used to investigate Ca^{2+} entry during Ca^{2+} oscillations, also in cells that express connexins (92–94), but these trivalent ions also inhibit hemichannels (31, 95, 96). In conclusion, connexin hemichannels may contribute to Ca^{2+} oscillations in connexin-expressing cells. Interestingly, connexin-expressing cells may also display hemichannel-independent Ca^{2+} oscillations, as exemplified here with ATP. This differential contribution of hemichannels to Ca^{2+} oscillations may result in distinct downstream response patterns to this fundamental cell signal, as recently observed in brain endothelial cells (34).

Acknowledgments—We gratefully thank Dr. C. C. Naus for supplying C6 glioma cells and Dr. D. F. Boehning for sharing the IP_3RCYT peptide. Special thanks go to K. Leurs, E. Tack, C. Mabilde, T. Vanthuyne, B. Blanckaert, and M. Yüksel for outstanding technical support.

REFERENCES

1. Case, R. M., Eisner, D., Gurney, A., Jones, O., Muallem, S., and Verkhratsky, A. (2007) Evolution of calcium homeostasis. from birth of the first cell to an omnipresent signaling system. *Cell Calcium* **42,** 345–350
2. Dupont, G., Combettes, L., and Leybaert, L. (2007) Calcium dynamics. Spatio-temporal organization from the subcellular to the organ level. *Int. Rev. Cytol.* **261,** 193–245
3. Berridge, M. J., Lipp, P., and Bootman, M. D. (2000) The versatility and universality of calcium signaling. *Nat. Rev. Mol. Cell Biol.* **1,** 11–21
4. Berridge, M. J., Bootman, M. D., and Roderick, H. L. (2003) Calcium signaling. Dynamics, homeostasis, and remodeling. *Nat. Rev. Mol. Cell Biol.* **4,** 517–529
5. Putney, J. W., and Bird, G. S. (2008) Cytoplasmic calcium oscillations and store-operated calcium influx. *J. Physiol.* **586,** 3055–3059
6. Uhlén, P., and Fritz, N. (2010) Biochemistry of calcium oscillations. *Biochem. Biophys. Res. Commun.* **396,** 28–32
7. Bezprozvanny, I., Watras, J., and Ehrlich, B. E. (1991) Bell-shaped calcium-response curves of Ins(1,4,5)P_3- and calcium-gated channels from endoplasmic reticulum of cerebellum. *Nature* **351,** 751–754
8. Keizer, J., and De Young, G. W. (1992) Two roles of Ca^{2+} in agonist stimulated Ca^{2+} oscillations. *Biophys. J.* **61,** 649–660
9. Goldbeter, A., Dupont, G., and Berridge, M. J. (1990) Minimal model for signal-induced Ca^{2+} oscillations and for their frequency encoding through protein phosphorylation. *Proc. Natl. Acad. Sci. U.S.A.* **87,** 1461–1465
10. Sneyd, J., Keizer, J., and Sanderson, M. J. (1995) Mechanisms of calcium oscillations and waves. A quantitative analysis. *FASEB J.* **9,** 1463–1472
11. Young, K. W., Nash, M. S., Challiss, R. A., and Nahorski, S. R. (2003) Role of Ca^{2+} feedback on single cell inositol 1,4,5-trisphosphate oscillations mediated by G-protein-coupled receptors. *J. Biol. Chem.* **278,** 20753–20760
12. Politi, A., Gaspers, L. D., Thomas, A. P., and Höfer, T. (2006) Models of IP_3 and Ca^{2+} oscillations. Frequency encoding and identification of underlying feedbacks. *Biophys. J.* **90,** 3120–3133
13. Parker, I., and Ivorra, I. (1990) Inhibition by Ca^{2+} of inositol trisphosphate-mediated Ca^{2+} liberation. A possible mechanism for oscillatory release of Ca^{2+}. *Proc. Natl. Acad. Sci. U.S.A.* **87,** 260–264
14. Dawson, A. P. (1997) Calcium signaling. How do IP_3 receptors work? *Curr. Biol.* **7,** R544–R547
15. Hajnóczky, G., and Thomas, A. P. (1997) Minimal requirements for calcium oscillations driven by the IP_3 receptor. *EMBO J.* **16,** 3533–3543
16. Rebecchi, M. J., and Pentyala, S. N. (2000) Structure, function, and control of phosphoinositide-specific phospholipase C. *Physiol. Rev.* **80,** 1291–1335
17. Fukami, K., Inanobe, S., Kanemaru, K., and Nakamura, Y. (2010) Phospholipase C is a key enzyme regulating intracellular calcium and modulating the phosphoinositide balance. *Prog. Lipid Res.* **49,** 429–437
18. Nash, M. S., Young, K. W., Challiss, R. A., and Nahorski, S. R. (2001) Intracellular signaling. Receptor-specific messenger oscillations. *Nature* **413,** 381–382
19. Thore, S., Dyachok, O., and Tengholm, A. (2004) Oscillations of phospholipase C activity triggered by depolarization and Ca^{2+} influx in insulin-secreting cells. *J. Biol. Chem.* **279,** 19396–19400
20. Thomas, A. P., Bird, G. S., Hajnóczky, G., Robb-Gaspers, L. D., and Putney, J. W., Jr. (1996) Spatial and temporal aspects of cellular calcium signaling. *FASEB J.* **10,** 1505–1517
21. Reetz, G., and Reiser, G. (1996) $[Ca^{2+}]_i$ oscillations induced by bradykinin in rat glioma cells associated with Ca^{2+} store-dependent Ca^{2+} influx are controlled by cell volume and by membrane potential. *Cell Calcium* **19,** 143–156
22. Shuttleworth, T. J., and Mignen, O. (2003) Calcium entry and the control of calcium oscillations. *Biochem. Soc. Trans.* **31,** 916–919
23. Jones, B. F., Boyles, R. R., Hwang, S. Y., Bird, G. S., and Putney, J. W. (2008) Calcium influx mechanisms underlying calcium oscillations in rat hepatocytes. *Hepatology* **48,** 1273–1281
24. Sacks, R. S., Firth, A. L., Remillard, C. V., Agange, N., Yau, J., Ko, E. A., and Yuan, J. X. (2008) Thrombin-mediated increases in cytosolic Ca^{2+} involve different mechanisms in human pulmonary artery smooth muscle and endothelial cells. *Am. J. Physiol. Lung Cell Mol. Physiol.* **295,** 1048–1055
25. Dupont, G., Combettes, L., Bird, G. S., and Putney, J. W. (2011) Calcium oscillations. *Cold Spring Harb. Perspect. Biol.* **3,** pii: a004226
26. Loewenstein, W. R. (1981) Junctional intercellular communication. The cell-to-cell membrane channel. *Physiol. Rev.* **61,** 829–913
27. Alexander, D. B., and Goldberg, G. S. (2003) Transfer of biologically important molecules between cells through gap junction channels. *Curr. Med. Chem.* **10,** 2045–2058
28. Kawano, S., Otsu, K., Kuruma, A., Shoji, S., Yanagida, E., Muto, Y., Yoshikawa, F., Hirayama, Y., Mikoshiba, K., and Furuichi, T. (2006) ATP autocrine/paracrine signaling induces calcium oscillations and NFAT activation in human mesenchymal stem cells. *Cell Calcium* **39,** 313–324
29. Verma, V., Hallett, M. B., Leybaert, L., Martin, P. E., and Evans, W. H. (2009) Perturbing plasma membrane hemichannels attenuates calcium signaling in cardiac cells and HeLa cells expressing connexins. *Eur. J. Cell Biol.* **88,** 79–90
30. Braet, K., Vandamme, W., Martin, P. E., Evans, W. H., and Leybaert, L. (2003) Photoliberating inositol-1,4,5-trisphosphate triggers ATP release that is blocked by the connexin mimetic peptide gap 26. *Cell Calcium* **33,** 37–48
31. Braet, K., Aspeslagh, S., Vandamme, W., Willecke, K., Martin, P. E., Evans, W. H., and Leybaert, L. (2003) Pharmacological sensitivity of ATP release triggered by photoliberation of inositol-1,4,5-trisphosphate and zero extracellular calcium in brain endothelial cells. *J. Cell Physiol.* **197,** 205–213
32. Leybaert, L., Braet, K., Vandamme, W., Cabooter, L., Martin, P. E., and Evans, W. H. (2003) Connexin channels, connexin mimetic peptides and ATP release. *Cell Commun. Adhes.* **10,** 251–257
33. Evans, W. H., De Vuyst, E., and Leybaert, L. (2006) The gap junction cellular internet. Connexin hemichannels enter the signaling limelight. *Biochem. J.* **397,** 1–14
34. De Bock, M., Culot, M., Wang, N., Bol, M., Decrock, E., De Vuyst, E., da Costa, A., Dauwe, I., Vinken, M., Simon, A. M., Rogiers, V., De Ley, G., Evans, W. H., Bultynck, G., Dupont, G., Cecchelli, R., and Leybaert, L. (2011) Connexin channels provide a target to manipulate brain endothelial calcium dynamics and blood-brain barrier permeability. *J. Cereb. Blood Flow Metab.* **31,** 1942–1957
35. De Vuyst, E., Decrock, E., Cabooter, L., Dubyak, G. R., Naus, C. C., Evans, W. H., and Leybaert, L. (2006) Intracellular calcium changes trigger connexin 32 hemichannel opening. *EMBO J.* **25,** 34–44
36. De Vuyst, E., Wang, N., Decrock, E., De Bock, M., Vinken, M., Van Moorhem, M., Lai, C., Culot, M., Rogiers, V., Cecchelli, R., Naus, C. C., Evans, W. H., and Leybaert, L. (2009) Ca^{2+} regulation of connexin 43 hemichannels in C6 glioma and glial cells. *Cell Calcium* **46,** 176–187
37. Ponsaerts, R., De Vuyst, E., Retamal, M., D'hondt, C., Vermeire, D., Wang, N., De Smedt, H., Zimmermann, P., Himpens, B., Vereecke, J., Leybaert, L., and Bultynck, G. (2010) Intramolecular loop/tail interactions are essential for connexin 43-hemichannel activity. *FASEB J.* **24,** 4378–4395

38. Boehning, D., van Rossum, D. B., Patterson, R. L., and Snyder, S. H. (2005) A peptide inhibitor of cytochrome *c*/inositol 1,4,5-trisphosphate receptor binding blocks intrinsic and extrinsic cell death pathways. *Proc. Natl. Acad. Sci. U.S.A.* **102,** 1466–1471
39. Grynkiewicz, G., Poenie, M., and Tsien, R. Y. (1985) A new generation of Ca^{2+} indicators with greatly improved fluorescence properties. *J. Biol. Chem.* **260,** 3440–3450
40. Van Moorhem, M., Decrock, E., Coussee, E., Faes, L., De Vuyst, E., Vranckx, K., De Bock, M., Wang, N., D'Herde, K., Lambein, F., Callewaert, G., and Leybaert, L. (2010) L-β-ODAP alters mitochondrial Ca^{2+} handling as an early event in excitotoxicity. *Cell Calcium* **47,** 287–296
41. De Vuyst, E., De Bock, M., Decrock, E., Van Moorhem, M., Naus, C., Mabilde, C., and Leybaert, L. (2008) *In situ* bipolar electroporation for localized cell loading with reporter dyes and investigating gap junctional coupling. *Biophys. J.* **94,** 469–479
42. Decrock, E., De Vuyst, E., Vinken, M., Van Moorhem, M., Vranckx, K., Wang, N., Van Laeken, L., De Bock, M., D'Herde, K., Lai, C. P., Rogiers, V., Evans, W. H., Naus, C. C., and Leybaert, L. (2009) Connexin 43 hemichannels contribute to the propagation of apoptotic cell death in a rat C6 glioma cell model. *Cell Death Differ.* **16,** 151–163
43. Anselmi, F., Hernandez, V. H., Crispino, G., Seydel, A., Ortolano, S., Roper, S. D., Kessaris, N., Richardson, W., Rickheit, G., Filippov, M. A., Monyer, H., and Mammano, F. (2008) ATP release through connexin hemichannels and gap junction transfer of second messengers propagate Ca^{2+} signals across the inner ear. *Proc. Natl. Acad. Sci. U.S.A.* **105,** 18770–18775
44. Iyer, S., Deutsch, K., Yan, X., and Lin, B. (2007) Batch RNAi selector. A stand-alone program to predict specific siRNA candidates in batches with enhanced sensitivity. *Comput. Methods Programs Biomed* **85,** 203–209
45. Sneyd, J., Tsaneva-Atanasova, K., Reznikov, V., Bai, Y., Sanderson, M. J., and Yule, D. I. (2006) A method for determining the dependence of calcium oscillations on inositol trisphosphate oscillations. *Proc. Natl. Acad. Sci. U.S.A.* **103,** 1675–1680
46. Swann, K., and Yu, Y. (2008) The dynamics of calcium oscillations that activate mammalian eggs. *Int. J. Dev. Biol.* **52,** 585–594
47. Pelegrin, P., and Surprenant, A. (2006) Pannexin-1 mediates large pore formation and interleukin-1β release by the ATP-gated P2X7 receptor. *EMBO J.* **25,** 5071–5082
48. Vinken, M., Decrock, E., De Vuyst, E., De Bock, M., Vandenbroucke, R. E., De Geest, B. G., Demeester, J., Sanders, N. N., Vanhaecke, T., Leybaert, L., and Rogiers, V. (2010) Connexin32 hemichannels contribute to the apoptotic-to-necrotic transition during Fas-mediated hepatocyte cell death. *Cell Mol. Life Sci.* **67,** 907–918
49. De Blasio, B. F., Røttingen, J. A., Sand, K. L., Giaever, I., and Iversen, J. G. (2004) Global, synchronous oscillations in cytosolic calcium and adherence in bradykinin-stimulated Madin-Darby canine kidney cells. *Acta Physiol. Scand.* **180,** 335–346
50. Bindschadler, M., and Sneyd, J. (2001) A bifurcation analysis of two coupled calcium oscillators. *Chaos* **11,** 237–246
51. Koizumi, S. (2010) Synchronization of Ca^{2+} oscillations. Involvement of ATP release in astrocytes. *FEBS J.* **277,** 286–292
52. Easton, A. S., and Abbott, N. J. (2002) Bradykinin increases permeability by calcium and 5-lipoxygenase in the ECV304/C6 cell culture model of the blood-brain barrier. *Brain Res.* **953,** 157–169
53. Kennedy, C., Proulx, P. R., and Hébert, R. L. (1997) Bradykinin-induced translocation of cytoplasmic phospholipase A2 in MDCK cells. *Can J. Physiol. Pharmacol.* **75,** 563–567
54. Gómez-Hernández, J. M., de Miguel, M., Larrosa, B., González, D., and Barrio, L. C. (2003) Molecular basis of calcium regulation in connexin-32 hemichannels. *Proc. Natl. Acad. Sci. U.S.A.* **100,** 16030–16035
55. Thimm, J., Mechler, A., Lin, H., Rhee, S., and Lal, R. (2005) Calcium-dependent open/closed conformations and interfacial energy maps of reconstituted hemichannels. *J. Biol. Chem.* **280,** 10646–10654
56. Ye, Z. C., Wyeth, M. S., Baltan-Tekkok, S., and Ransom, B. R. (2003) Functional hemichannels in astrocytes. A novel mechanism of glutamate release. *J. Neurosci.* **23,** 3588–3596
57. Stridh, M. H., Tranberg, M., Weber, S. G., Blomstrand, F., and Sandberg, M. (2008) Stimulated efflux of amino acids and glutathione from cultured hippocampal slices by omission of extracellular calcium. Likely involvement of connexin hemichannels. *J. Biol. Chem.* **283,** 10347–10356
58. Boehning, D., Patterson, R. L., Sedaghat, L., Glebova, N. O., Kurosaki, T., and Snyder, S. H. (2003) Cytochrome *c* binds to inositol (1,4,5) trisphosphate receptors, amplifying calcium-dependent apoptosis. *Nat. Cell Biol.* **5,** 1051–1061
59. Szalai, G., Krishnamurthy, R., and Hajnóczky, G. (1999) Apoptosis driven by IP_3-linked mitochondrial calcium signals. *EMBO J.* **18,** 6349–6361
60. Pacher, P., and Hajnóczky, G. (2001) Propagation of the apoptotic signal by mitochondrial waves. *EMBO J.* **20,** 4107–4121
61. Boehning, D., Patterson, R. L., and Snyder, S. H. (2004) Apoptosis and calcium. New roles for cytochrome *c* and inositol 1,4,5-trisphosphate. *Cell Cycle* **3,** 252–254
62. Colosetti, P., Tunwell, R. E., Cruttwell, C., Arsanto, J. P., Mauger, J. P., and Cassio, D. (2003) The type 3 inositol 1,4,5-trisphosphate receptor is concentrated at the tight junction level in polarized MDCK cells. *J. Cell Sci.* **116,** 2791–2803
63. Monaco, G., Decrock, E., Akl, H., Ponsaerts, R., Vervliet, T., Luyten, T., De Maeyer, M., Missiaen, L., Distelhorst, C. W., De Smedt, H., Parys, J. B., Leybaert, L., and Bultynck, G. (2012) Selective regulation of IP_3 receptor-mediated Ca^{2+} signaling and apoptosis by the BH4 domain of Bcl-2 versus Bcl-Xl. *Cell Death Differ* **19,** 295–309
64. Giepmans, B. N., and Moolenaar, W. H. (1998) The gap junction protein connexin43 interacts with the second PDZ domain of the zona occludens-1 protein. *Curr. Biol.* **8,** 931–934
65. Hunter, A. W., Barker, R. J., Zhu, C., and Gourdie, R. G. (2005) Zonula occludens-1 alters connexin43 gap junction size and organization by influencing channel accretion. *Mol. Biol. Cell* **16,** 5686–5698
66. O'Quinn, M. P., Palatinus, J. A., Harris, B. S., Hewett, K. W., and Gourdie, R. G. (2011) A peptide mimetic of the connexin43 carboxyl terminus reduces gap junction remodeling and induced arrhythmia after ventricular injury. *Circ. Res.* **108,** 704–715
67. Tai, C. J., Kang, S. K., and Leung, P. C. (2001) Adenosine triphosphate-evoked cytosolic calcium oscillations in human granulosa-luteal cells. Role of protein kinase C. *J. Clin. Endocrinol. Metab.* **86,** 773–777
68. Bergner, A., and Sanderson, M. J. (2002) ATP stimulates Ca^{2+} oscillations and contraction in airway smooth muscle cells of mouse lung slices. *Am. J. Physiol. Lung Cell Mol. Physiol.* **283,** L1271–L1279
69. Berridge, M. J., Cobbold, P. H., and Cuthbertson, K. S. (1988) Spatial and temporal aspects of cell signaling. *Philos. Trans. R Soc. Lond B Biol. Sci.* **320,** 325–343
70. Davis, R. J., Challiss, J., and Nahorski, S. R. (1999) Enhanced purinoceptor-mediated Ca^{2+} signaling in L-fibroblasts overexpressing type 1 inositol 1,4,5-trisphosphate receptors. *Biochem. J.* **341,** 813–820
71. Røttingen, J. A., Camerer, E., Mathiesen, I., Prydz, H., and Iversen, J. G. (1997) Synchronized Ca^{2+} oscillations induced in Madin-Darby canine kidney cells by bradykinin and thrombin but not by ATP. *Cell Calcium* **21,** 195–211
72. Sage, S. O., Adams, D. J., and van Breemen, C. (1989) Synchronized oscillations in cytoplasmic free calcium concentration in confluent bradykinin-stimulated bovine pulmonary artery endothelial cell monolayers. *J. Biol. Chem.* **264,** 6–9
73. Carter, T. D., Bogle, R. G., and Bjaaland, T. (1991) Spiking of intracellular calcium ion concentration in single cultured pig aortic endothelial cells stimulated with ATP or bradykinin. *Biochem. J.* **278,** 697–704
74. De Blasio, B. F., Iversen, J. G., and Røttingen, J. A. (2004) Intercellular calcium signaling in cultured renal epithelia. A theoretical study of synchronization mode and pacemaker activity. *Eur. Biophys. J.* **33,** 657–670
75. Nash, M. S., Schell, M. J., Atkinson, P. J., Johnston, N. R., Nahorski, S. R., and Challiss, R. A. (2002) Determinants of metabotropic glutamate receptor-5-mediated Ca^{2+} and inositol 1,4,5-trisphosphate oscillation frequency. Receptor density *versus* agonist concentration. *J. Biol. Chem.* **277,** 35947–35960
76. Bird, G. S., Rossier, M. F., Obie, J. F., and Putney, J. W., Jr. (1993) Sinusoidal oscillations in intracellular calcium requiring negative feedback by protein kinase C. *J. Biol. Chem.* **268,** 8425–8428
77. Boarder, M. R., and Challiss, R. A. (1992) Role of protein kinase C in the regulation of histamine- and bradykinin-stimulated inositol polyphos-

phate turnover in adrenal chromaffin cells. *Br. J. Pharmacol.* **107,** 1140–1145
78. Willars, G. B., Müller-Esterl, W., and Nahorski, S. R. (1999) Receptor phosphorylation does not mediate cross-talk between muscarinic M(3) and bradykinin B(2) receptors. *Am. J. Physiol.* **277,** C859–C869
79. Clarke, T. C., Williams, O. J., Martin, P. E., and Evans, W. H. (2009) ATP release by cardiac myocytes in a simulated ischemia model. Inhibition by a connexin mimetic and enhancement by an antiarrhythmic peptide. *Eur. J. Pharmacol.* **605,** 9–14
80. Zhang, S. W., Liu, Y., Huang, G. Z., and Liu, L. (2007) Aconitine alters connexin43 phosphorylation status and Ca^{2+} oscillation patterns in cultured ventricular myocytes of neonatal rats. *Toxicol. In Vitro* **21,** 1476–1485
81. Romanov, R. A., Rogachevskaja, O. A., Bystrova, M. F., Jiang, P., Margolskee, R. F., and Kolesnikov, S. S. (2007) Afferent neurotransmission mediated by hemichannels in mammalian taste cells. *EMBO J.* **26,** 657–667
82. Schalper, K. A., Sánchez, H. A., Lee, S. C., Altenberg, G. A., Nathanson, M. H., and Sáez, J. C. (2010) Connexin 43 hemichannels mediate the Ca^{2+} influx induced by extracellular alkalinization. *Am. J. Physiol. Cell Physiol.* **299,** C1504–C1515
83. Sánchez, H. A., Orellana, J. A., Verselis, V. K., and Sáez, J. C. (2009) Metabolic inhibition increases activity of connexin-32 hemichannels permeable to Ca^{2+} in transfected HeLa cells. *Am. J. Physiol. Cell Physiol.* **297,** C665–C678
84. Shintani-Ishida, K., Uemura, K., and Yoshida, K. (2007) Hemichannels in cardiomyocytes open transiently during ischemia and contribute to reperfusion injury after brief ischemia. *Am. J. Physiol. Heart Circ. Physiol.* **293,** H1714–H1720
85. Shuttleworth, T. J. (1999) What drives calcium entry during $[Ca^{2+}]_i$ oscillations? Challenging the capacitative model. *Cell Calcium* **25,** 237–246
86. Martin, S. C., and Shuttleworth, T. J. (1994) Ca^{2+} influx drives agonist-activated $[Ca^{2+}]_i$ oscillations in an exocrine cell. *FEBS Lett.* **352,** 32–36
87. Shuttleworth, T. J., and Thompson, J. L. (1996) Ca^{2+} entry modulates oscillation frequency by triggering Ca^{2+} release. *Biochem. J.* **313,** 815–819
88. Meyer, T., and Stryer, L. (1988) Molecular model for receptor-stimulated calcium spiking. *Proc. Natl. Acad. Sci. U.S.A.* **85,** 5051–5055
89. Fioretti, B., Franciolini, F., and Catacuzzeno, L. (2005) A model of intracellular Ca^{2+} oscillations based on the activity of the intermediate-conductance Ca^{2+}-activated K+ channels. *Biophys. Chem* **113,** 17–23
90. Maruyama, T., Kanaji, T., Nakade, S., Kanno, T., and Mikoshiba, K. (1997) 2APB, 2-aminoethoxydiphenyl borate, a membrane-penetrable modulator of Ins(1,4,5)P_3-induced Ca^{2+} release. *J. Biochem.* **122,** 498–505
91. Tao, L., and Harris, A. L. (2007) 2-Aminoethoxydiphenyl borate directly inhibits channels composed of connexin26 and/or connexin32. *Mol. Pharmacol.* **71,** 570–579
92. Hu, R., He, M. L., Hu, H., Yuan, B. X., Zang, W. J., Lau, C. P., Tse, H. F., and Li, G. R. (2009) Characterization of calcium signaling pathways in human preadipocytes. *J. Cell. Physiol.* **220,** 765–770
93. Estrada, M., Espinosa, A., Gibson, C. J., Uhlen, P., and Jaimovich, E. (2005) Capacitative calcium entry in testosterone-induced intracellular calcium oscillations in myotubes. *J. Endocrinol.* **184,** 371–379
94. Pizzo, P., Burgo, A., Pozzan, T., and Fasolato, C. (2001) Role of capacitative calcium entry on glutamate-induced calcium influx in type-I rat cortical astrocytes. *J. Neurochem.* **79,** 98–109
95. Contreras, J. E., Sáez, J. C., Bukauskas, F. F., and Bennett, M. V. (2003) Gating and regulation of connexin 43 (Cx43) hemichannels. *Proc. Natl. Acad. Sci. U.S.A.* **100,** 11388–11393
96. Retamal, M. A., Froger, N., Palacios-Prado, N., Ezan, P., Sáez, P. J., Sáez, J. C., and Giaume, C. (2007) Cx43 hemichannels and gap junction channels in astrocytes are regulated oppositely by proinflammatory cytokines released from activated microglia. *J. Neurosci.* **27,** 13781–13792
97. Tu, H., Wang, Z., and Bezprozvanny, I. (2005) Modulation of mammalian inositol 1,4,5-trisphosphate receptor isoforms by calcium. A role of calcium sensor region. *Biophys. J.* **88,** 1056–1069